

3 The Precambrian paleogeography of Laurentia

Nicholas L. Swanson-Hysell¹

¹ Department of Earth and Planetary Science, University of California, Berkeley, CA 94720 USA

This chapter is in preparation for the book Ancient Supercontinents and the Paleogeography of the Earth

¹ **3.1 Introduction**

Laurentia was a major continent throughout the majority of the Proterozoic and is hypothesized to have had a central position in both the Paleoproterozoic Nuna and Neoproterozoic Rodinia supercontinents. The paleogeographic position of Laurentia is key to the development of reconstructions of Proterozoic paleogeography. There is a rich record of Precambrian paleomagnetic poles from Laurentia as well as an extensive geologic history of tectonism that are both key to evaluating and developing paleogeographic models. This chapter seeks to provide a concise review of these records.

⁹ **3.2 Broad tectonic history overview**

Laurentia refers to the craton that forms the Precambrian core of North America (Fig. 1). Laurentia is comprised of multiple Archean provinces that had unique histories prior to their amalgamation in the Paleoproterozoic, as well as tectonic zones of crustal growth that post-date this assembly (Hoffman, 1989; Whitmeyer and Karlstrom, 2007). Collision between the Superior province and the composite Slave+Rae+Hearne provinces that resulted in the Trans-Hudson orogeny represents a major event in the formation of Laurentia (Corrigan et al., 2009). Terminal collision recorded in the Trans-Hudson orogen is estimated to have been ca. 1.86 to 1.82 Ga based on constraints such as U-Pb dating of monazite grains and zircon rims (Skipton et al., 2016; Weller and St-Onge, 2017, e.g.). A period of accretionary and collision orogenesis is recorded in the constituent provinces and terranes of Laurentia leading up to the terminal collision of the

20 Trans-Hudson orogeny. This overall story of rapid Paleoproterozoic amalgamation of Laurentia's
21 constituent Archean provinces, including the terminal Trans-Hudson orogeny, was synthesized in
22 the seminal *United Plates of America* paper of Hoffman (1988) and has been refined in the time
23 since – particularly with additional geochronological constraints. Of most relevance here are the
24 events that led to the suturing of more major Archean provinces: the Thelon orogen associated
25 with the collision between the Slave and Rae provinces ca. 2.0 to 1.9 Ga (Hoffman, 1989); the
26 Snowbird orogen associated with ca. 1.89 Ga collision between the Rae and Hearne provinces and
27 associated terranes (Berman et al., 2007); the Nagssugtoqidian orogen due to the ca. 1.86 to 1.84
28 Ga collision between the Rae and North Atlantic provinces (St-Onge et al., 2009); and the
29 Torngat orogen resulting from the ca. 1.87 to 1.85 Ga collision of the Meta Incognita province
30 (grouped with the Rae province in older compilations) with the North Atlantic province (St-Onge
31 et al., 2009). As for the Wyoming province, many models posit that it was conjoined with Hearne
32 and associated provinces at the time of the Trans-Hudson orogeny (e.g. St-Onge et al., 2009;
33 Pehrsson et al., 2015) or was proximal to Hearne and Superior while still undergoing continued
34 translation up to ca. 1.80 Ga (Whitmeyer and Karlstrom, 2007). A contrasting view has been
35 proposed that the Wyoming province and Medicine Hat blocks was not conjoined with the
36 other Laurentia provinces until ca. 1.72 Ga (Kilian et al., 2016). This interpretation is argued to
37 be consistent with geochronological constraints on monazite and metamorphic zircon indicating
38 active collisional orogenesis associated with the Big Sky orogen on the northern margin of the
39 craton as late as ca. 1.75 to 1.72 Ga (Condit et al., 2015) and ca. 1.72 tectonomagmatic activity
40 in the Black Hills region (Redden et al., 1990). However, the evidence for earlier orogenesis ca.
41 1.78 to 1.75 in the Black Hills (Dahl et al., 1999; Hrncir et al., 2017), as well as high-grade
42 tectonism as early as ca. 1.81 Ga in the Big Sky orogen (Condit et al., 2015), may support the
43 interpretation of Hrncir et al. (2017) that ca. 1.72 Ga activity is a minor overprint on ca. 1.75
44 terminal suturing between Wyoming and Superior. Regardless, in both of these interpretations,
45 Wyoming is a later addition to Laurentia with final suturing post-dating ca. 1.82 Ga
46 amalgamation of Archean provinces with the Trans-Hudson orogen further to the northeast.
47 Overall, the collision of these Archean microcontinents between ca. 1.9 and 1.8 Ga lead to rapid
48 amalgamation of the majority of the Laurentia craton.

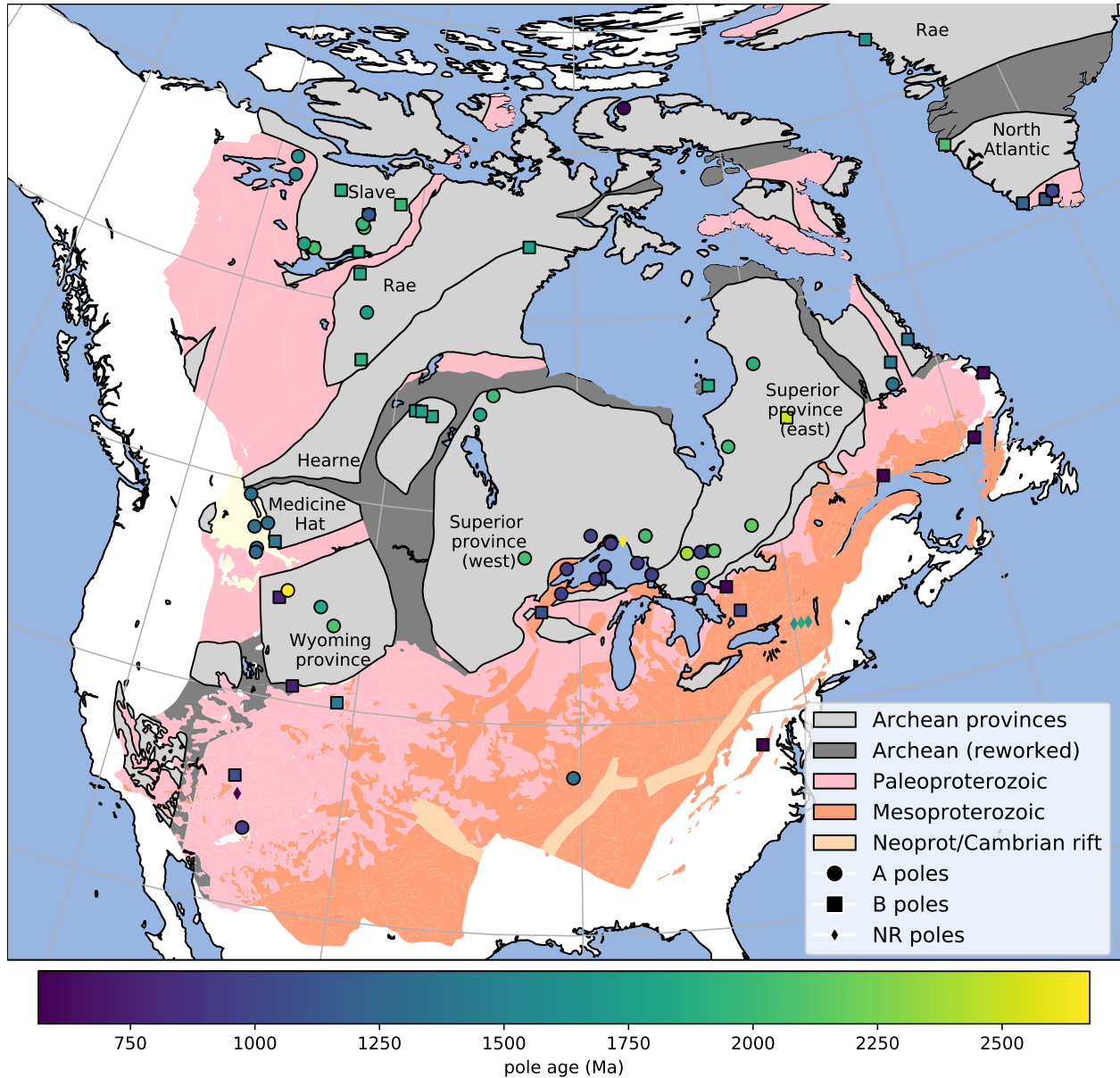


Figure 1. Simplified map of Laurentia showing the location of Archean provinces (labeled with text) and younger Paleoproterozoic and Mesoproterozoic crust (simplified from Whitmeyer and Karlstrom, 2007 with additions for Greenland based on St-Onge et al., 2009). The localities from which the compiled Precambrian paleomagnetic poles were developed are shown and colored by age. The circles (A rated poles) and squares (B rated poles) have been assessed by the Nordic workshop panel.

49 Crustal growth also progressed in the Paleoproterozoic through accretionary orogenesis. This
50 accretion occurred within the Wopmay orogen through ca. 1.88 Ga arc-continent collision that led
51 to the accretion of the Hottah terrane (the Calderian orogeny) and the subsequent emplacement
52 of the Great Bear magmatic zone from ca. 1.88 to 1.84 Ga (Hildebrand et al., 2009). Coeval with
53 the Trans-Hudson orogeny was the peripheral Penokean orogeny during which both microcontinent
54 blocks (the Marshfield terrane) and arc terranes accreted on the southeastern margin of the west
55 Superior province ca. 1.86 to 1.82 (Schulz and Cannon, 2007). Firm evidence of the end of the
56 orogeny comes from the ca. 1.78 undeformed plutons of the post-Penokean East Central
57 Minnesota Batholith (Holm et al., 2005).

58 In the paleogeographic model framework of Pehrsson et al. (2015), the collisions of provinces
59 and terranes leading up to the Trans-Hudson orogeny mark the initial phase of assembly of the
60 supercontinent Nuna. The Trans-Hudson orogeny itself is taken to be the terminal collision
61 associated with the closure of the Manikewan Ocean that had previous been a large oceanic tract
62 separating the Superior province from the composite Slave+Rae+Hearne+North Atlantic
63 provinces (often referred to as the Churchill domain or plate; e.g. Skipton et al., 2016; Weller and
64 St-Onge, 2017). The Pehrsson et al. (2015) model posits that this period terminal collision not
65 only resulted in the amalgamation of Laurentia, but is also associated with the assembly of the
66 supercontinent Nuna that is hypothesized to include other major Paleoproterozoic cratons
67 including Siberia, Congo/São Francisco, West Africa, and Amazonia (Whitmeyer and Karlstrom,
68 2007; Pehrsson et al., 2015).

69 Following the Trans-Hudson orogeny, the locus of orogenesis migrated to the exterior of
70 Laurentia. This change marks a shift in the predominant style of Laurentia's growth as subsequent
71 crustal growth occurred dominantly through accretion of juvenile crust along the southern and
72 eastern margin of the nucleus of Archean provinces (Whitmeyer and Karlstrom, 2007; Figs. 1 and
73 2). Determining the extent of these belts is complicated by poor exposure of them in the
74 midcontinent relative to the exposure of the Archean provinces throughout the Canadian shield.
75 Major growth of Laurentia following the amalgamation of these Archean provinces occurred
76 associated with the arc-continent collision of the ca. 1.71 to 1.68 Ga Yavapai orogeny. Yavapai
77 orogenesis is interpreted to have resulted from the accretion of a series of arc terranes that

78 collided with each other and Laurentia (Karlstrom et al., 2001). Yavapai accretion was followed
79 by widespread emplacement of granitoid intrusions (Whitmeyer and Karlstrom, 2007). These
80 intrusions are hypothesized to have stabilized the juvenile accreted terranes that subsequently
81 remained part of Laurentia (Whitmeyer and Karlstrom, 2007). Subsequent accretionary
82 orogenesis of the ca. 1.65–1.60 Ga Mazatzal Orogeny and associated plutonism lead to further
83 crustal growth in the latest Paleoproterozoic (Karlstrom and Bowring, 1988). Laurentia's growth
84 continued in the Mesoproterozoic along the southeast margin through further juvenile terrane and
85 arc accretion. An interval of major plutonism occurred ca. 1.48–1.35 Ga leading to the formation
86 of A-type granitoids throughout both Mesoproterozoic and Paleoproterozoic provinces extending
87 from the southwest United States up to the Central Gneiss Belt of Ontario to the northeast of
88 Georgian Bay (Slagstad et al., 2009). This plutonism is likely due to crustal melting within a
89 back-arc region of ca. 1.50 to 1.43 Ga accretionary orogenesis (Bickford et al., 2015). Younger
90 magmatic activity ca. 1.37 Ga of the Southern Granite–Rhyolite Province suggests a similar
91 tectonic setting of accretionary orogenesis at that time (Bickford et al., 2015). While an active
92 margin interpretation with magmatism in back-arc setting has gained traction within the
93 literature with additional data, the tectonic setting is often described as enigmatic given earlier
94 interpretations of an anorogenic setting (see references in Slagstad et al., 2009).

95 Accretionary orogenesis continued along the (south)east margin of Laurentia with the
96 arc-continent collision of the ca. 1.25-1.22 Ga Elzevirian orogeny (McLelland et al., 2013). The
97 subsequent ca. 1.19 to 1.16 Ga Shawinigan orogeny is interpreted to be due to the accretion of a
98 terrane comprised of amalgamated arc volcanics and associated metasediments and is followed by
99 a period of tectonic quiescence on the eastern margin of Laurentia until the collision orogenesis of
100 the Grenvillian orogeny (McLelland et al., 2010). In the latest Mesoproterozoic (ca. 1.11-1.08
101 Ga), a major intracontinental rift co-located with a large igneous province formed in Laurentia's
102 interior leading to extension within the Archean Superior province and Paleoproterozoic
103 provinces. This Midcontinent Rift lead to the formation of a thick succession of volcanics and
104 mafic intrusions that are well-preserved in Laurentia's interior. Midcontinent Rift development
105 ceased as major collisional orogenesis of the Grenvillian orogeny began (Swanson-Hysell et al.,
106 2019). The Grenvillian orogeny was a protracted interval of continent-continent collision (ca. 1.09

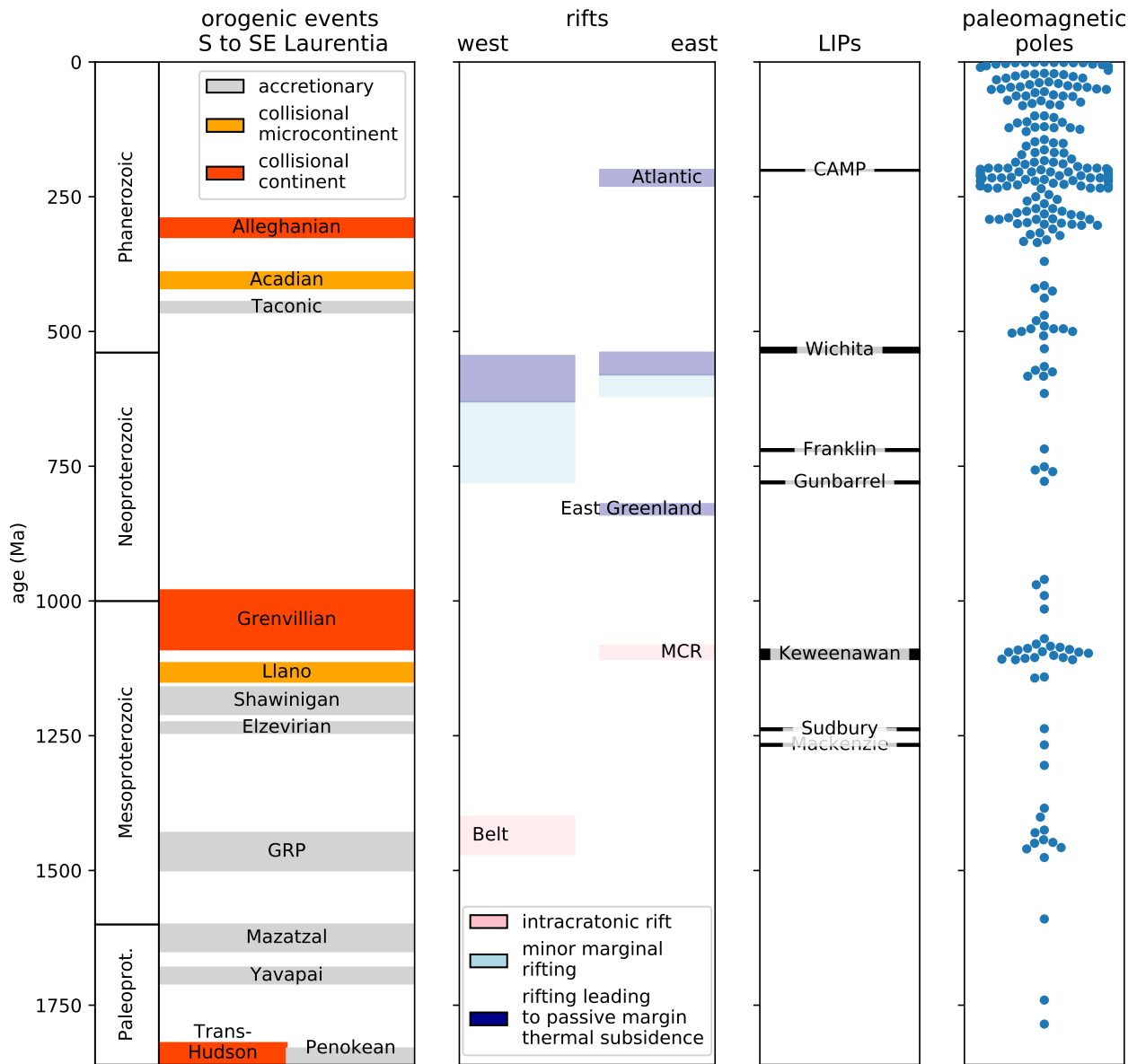


Figure 2. Simplified timeline of Laurentia's tectonic history over the past ~1.8 billion years. Brief summaries and references related to the orogenic and rifting episodes are given in the text. A timeline of large igneous provinces (LIPs) associated with typically brief and voluminous (or interpreted to be voluminous) volcanism is also shown. The interpreted age of paleomagnetic poles for Laurentia (not including separated terranes) compiled in this study for the Proterozoic and in Torsvik et al. (2012) for the Phanerozoic is shown.

¹⁰⁷ to 0.98 Ga) leading to amphibolite to granulite facies metamorphism through the orogen
¹⁰⁸ (McLlland et al., 2010). The orogeny is interpreted to have resulted in the development of a
¹⁰⁹ thick orogenic plateau (Rivers, 2008).

¹¹⁰ There is significantly less preserved crustal growth on the western margin of Laurentia (Fig. 1)
¹¹¹ and the Mesoproterozoic tectonic history is not as well elucidated as on the southern to eastern
¹¹² margin. The 15 to 20 km thick package of sedimentary rocks of the Belt-Purcell Supergroup is
¹¹³ associated with a ca. 1.47 to 1.40 intracontinental rift – the tectonic setting of which is debated.
¹¹⁴ Hoffman (1989) proposed that it may be a remanent back-arc basin trapped within a continent,
¹¹⁵ while others envision it as being associated with continental rifting along the margin associated
¹¹⁶ with separation of a conjugate continent (Jones et al., 2015). This region is interpreted to have
¹¹⁷ been subsequently deformed during a ca. 1.36 to 1.33 event known as the East Kootenay orogeny
¹¹⁸ (McMechan and Price, 1982; Nesheim et al., 2012; McFarlane, 2015).

¹¹⁹ This late Paleoproterozoic and Mesoproterozoic tectonic history provides significant
¹²⁰ constraints on paleogeographic reconstructions. In particular, the long-lived history of
¹²¹ accretionary orogenesis along the southeast (present-day coordinates) of Laurentia from the
¹²² initiation of the Yavapai orogeny (ca. 1.71 Ga) to the end of the Shawinigan orogeny (ca. 1.06
Ga) requires a long-lived open margin without a major conjugate continent up until the time of
¹²⁴ terminal Grenvillian orogeny collision (Karlstrom et al., 2001). This constraint is incorporated
¹²⁵ into models such as that of Zhang et al. (2012) and Pehrsson et al. (2015) which maintain a
¹²⁶ long-lived convergent margin throughout the Mesoproterozoic, but in some reconstructions other
¹²⁷ continental blocks are reconstructed into positions that are seemingly incompatible with this
¹²⁸ record of accretionary orogenesis (e.g. Amazonia in Elming et al., 2009). The high-grade
¹²⁹ metamorphism associated with the Ottawan phase of the Grenvillian orogeny itself requires a
¹³⁰ collision between Laurentia and (an)other continent(s) ca. 1080 Ma – the geological observation
¹³¹ of which first lead to the formulation of the hypothesis of the supercontinent Rodinia (Hoffman,
¹³² 1991). Evidence of large-scale continent-continent collision at the time of the Ottawan Phase of
¹³³ the Grenvillian orogeny is recorded in Texas, up through the Blue Ridge Appalachian inliers,
¹³⁴ through Ontario and up to the Labrador Sea. This extensive and major collision orogenic history
¹³⁵ recorded in Laurentia remains a strong piece of evidence that a supercontinent or

¹³⁶ (proto)supercontinent formed at the 1.0 Ga Mesoproterozoic to Neoproterozoic transition. The
¹³⁷ term Grenville orogeny or Grenville belt is used rather loosely throughout much of the literature
¹³⁸ to refer to any late Mesoproterozoic orogenic belt. The timeline of orogenesis on the Laurentia
¹³⁹ margin has more nuanced constraints than this which can be comparatively assessed when
¹⁴⁰ evaluating potential conjugate continents to Laurentia associated with the orogen (Fig. 2).

¹⁴¹ The subsequent Neoproterozoic tectonic history of Laurentia is dominantly a record of rifting
¹⁴² (Fig. 2). Along the western margin of Laurentia, small-scale rifting occurred ca. 780 to 720 Ma
¹⁴³ leading to deposition in basins that is recorded from the Death Valley region of SW Laurentia up
¹⁴⁴ to the Mackenzie Mountains of NW Laurentia (Macdonald et al., 2012; Rooney et al., 2017).
¹⁴⁵ However, this extensional basin development is relatively minor and predates the more significant
¹⁴⁶ rifting that lead to passive margin thermal subsidence that did not occur until the Ediacaran
¹⁴⁷ (closer to the ca. 539 Ma Neoproterozoic-Phanerozoic boundary; Bond et al., 1984; Levy and
¹⁴⁸ Christie-Blick, 1991). The emplacement of the ca. 780 Ma Gunbarrel large igneous province along
¹⁴⁹ this margin and the subsequent extension recorded in the basins is commonly interpreted to be
¹⁵⁰ associated with the break-up of Laurentia and a conjugate continent to the western margin. If
¹⁵¹ this interpretation is correct, it is unclear why there would be minimal thermal subsidence until
¹⁵² the Ediacaran (post 635 Ma as in Levy and Christie-Blick, 1991 and Witkosky and Wernicke,
¹⁵³ 2018). The geological evidence therefore supports active tectonism along the western margin of
¹⁵⁴ Laurentia, but suggests that more dramatic lithospheric thinning occurred later than the timing
¹⁵⁵ of rifting typically implemented in models of Rodinia break-up. One possibility, along the lines of
¹⁵⁶ that proposed in Ross (1991), is that ca. 780 Ma extensional tectonism is an inboard record of
¹⁵⁷ rifting and passive margin development that occurred further outboard. In this model,
¹⁵⁸ subsequent continent rifting that drove lithospheric thinning, perhaps associated with the
¹⁵⁹ departure of a microcontinent fragment rather than an already departed major conjugate
¹⁶⁰ continent, would be the cause of Ediacaran to Cambrian thermal subsidence. The margin that
¹⁶¹ did experience large-scale rifting and associated passive margin thermal subsidence earlier in the
¹⁶² Neoproterozoic is the northeast Greenland margin (Fig. 2). Available geochronological
¹⁶³ constraints and thermal subsidence modeling indicate ca. 820 Ma rifting followed by thermal
¹⁶⁴ subsidence of a stable platform (Maloof et al., 2006; Halverson et al., 2018). These data suggest

165 that conjugate continental lithosphere rifted away from northeast Greenland ca. 820 Ma.

166 Extensive rifting that was followed by thermal subsidence occurred along the southeast to east
167 Laurentia margin leading up to the Neoproterozoic-Phanerozoic boundary and is interpreted to be
168 associated with the opening of the Iapetus ocean. A record of this rifting is preserved as rift
169 basins that were part of failed arms (Rome trough, Reelfoot rift and Oklahoma aulacogen; Fig. 1)
170 as well as prolonged Cambrian to Ordovician passive margin thermal subsidence along the margin
171 (Bond et al., 1984; Whitmeyer and Karlstrom, 2007). The age of igneous intrusions that have
172 been interpreted to be rift-related play a significant role in interpretations of this history such as
173 in the rift development model of Burton and Southworth (2010). In this model,
174 spatially-restricted rifting occurs ca. 760 to 680 Ma in the region of modern-day North Carolina
175 and Virginia. Rifting ca. 620-580 Ma initiates in the region from modern-day New York to
176 Newfoundland and by ca. 580 to 550 Ma rifting extends along the length of Laurentia's eastern
177 margin. The last phases of this rifting appears to be associated with the separation of the
178 Argentine pre-Cordillera Cuyania terrane (Dickerson and Keller, 1998). Cuyania is widely
179 interpreted be a rifted fragment of SE Laurentia that separated associated with this early
180 Cambrian rifting and subsequently became part of Gondwana when it collided with other terranes
181 in the vicinity of the Rio de Plata craton during the Ordovician Famatinian orogeny (Martin
182 et al., 2019). As with other rifts, it is difficult to distinguish the separation of a cratonic fragment
183 as a microcontinent from the rifting of a major craton as the record that lingers on the craton is
184 similar. One interpretation is that there was successful break-up along the eastern margin during
185 the ca. 580 to 550 Ma interval of rifting prior to the ca. 539 Oklahoma aulacogen rifting that
186 liberated the Cuyania microcontinent. The Maz-Arequipa-Rio Apa (MARA) block with which
187 Cuyania collided (Martin et al., 2019) is likely a product of such rifting. Orogenesis between the
188 MARA block and the Rio de Plata and Kalahari in the ca. 530 Ma Pampean orogeny (Casquet
189 et al., 2018) predated the collision of Cuyania during the ca. 460 Famatinian orogeny in West
190 Gondwana (Rapalini, 2018).

191 The eastern margin of Laurentia then went through the cycle of Appalachian orogenesis. As is
192 visualized in Figure 2, there are parallels between the Grenville orogenic interval and the
193 Appalachian orogenic interval in that there was a period of arc-continent collision (Shawinigan

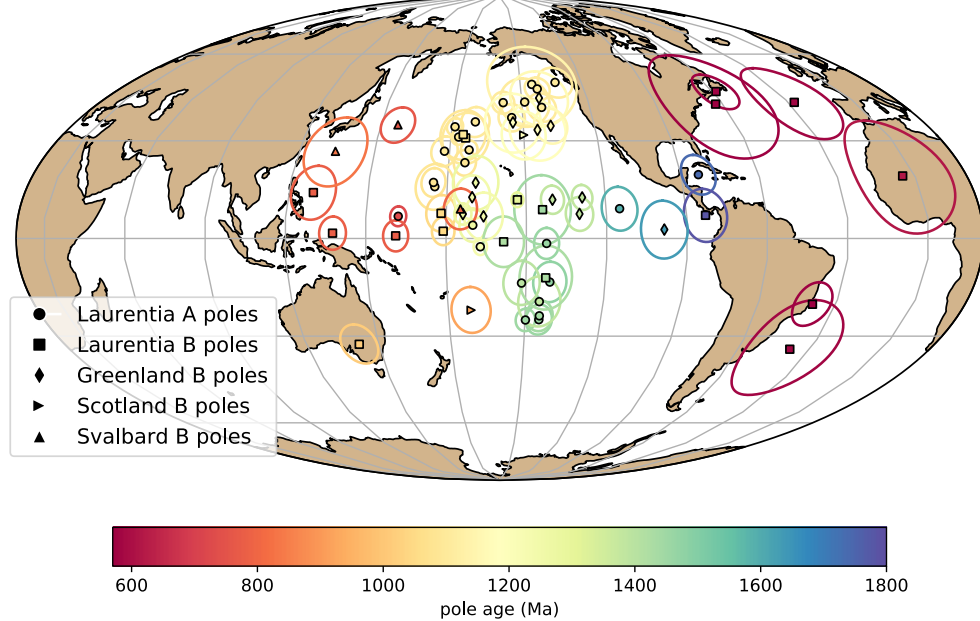
194 orogeny in the Grenville interval; Taconic orogeny in the Appalachian interval) followed by
195 microcontinent accretion (Llano in the Grenville interval; Acadian in the Appalachian interval)
196 that culminated in large-scale continent-continent collision (Grenvillian orogeny in the Grenville
197 interval; Alleghanian in the Appalachian interval). These similarities are the consequence of an
198 active margin facing an ocean basin that was progressively consumed until its consumption
199 resulted in continent-continent collision. In the case of the Grenville interval, this terminal
200 collision is interpreted to be associated with the assembly of the supercontinent Rodinia and in
201 the Appalachian interval it is interpreted to be associated with the assembly of the supercontinent
202 Pangea.

203 Even without considering other continents on Earth, the geological record of Paleoproterozoic
204 collisional of Archean provinces combined with accretionary orogenesis at that time and through
205 the rest of the Paleoproterozoic and Mesoproterozoic provides very strong evidence for mobile
206 plate tectonics driving Laurentia's evolution throughout the past 2 billion years. This tectonic
207 history inferred from geological data can be enhanced through integration with the paleomagnetic
208 record.

209 **3.3 Paleomagnetic pole compilation**

210 In this chapter, I focus on the compilation of paleomagnetic poles developed through the Nordic
211 Paleomagnetism Workshops with some additions and modifications (Fig. 3 and Table 2). The
212 Nordic Paleomagnetism Workshops have taken the approach of using expert panels to assess
213 paleomagnetic poles and assign them grades meant to convey the confidence that the community
214 has in these results (Evans et al., this volume). While many factors associated with
215 paleomagnetic poles can be assessed quantitatively through Fisher statistics and the precision of
216 geochronological constraints, other aspects such as the degree to which available field tests
217 constrain the magnetization to be primary require expert assessment. The categorizations used by
218 the expert panel are 'A' and 'B' with the last panel meeting occurring in Fall 2017 in Leirubakki,
219 Iceland. An 'A' rating refers to poles that are judged to be of such high-quality that they provide
220 essential constraints that should be satisfied in paleogeographic reconstructions. A 'B' rating is
221 associated with poles that are judged to likely provide a high-quality constraint, but have some

Poles for Laurentia (post-Paleoproterozoic amalgamation; with terranes)



Poles for Laurentia (pre-Paleoproterozoic amalgamation)

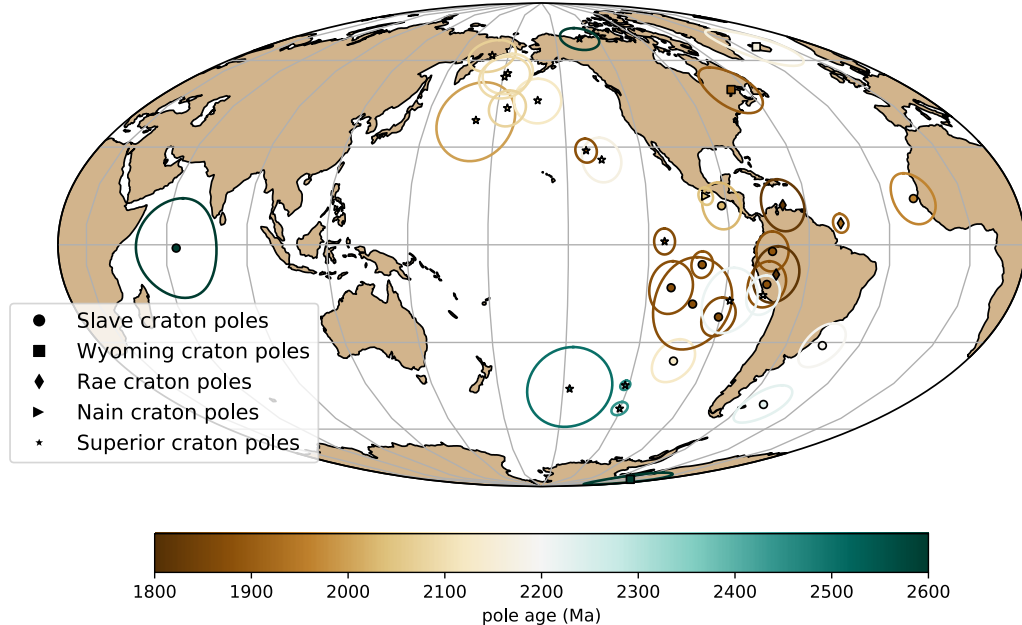


Figure 3. Top panel: Paleomagnetic poles from 1800 to 560 Ma for Laurentia (including Greenland, Scotland and Svalbard). Bottom panel: Paleomagnetic data for Archean Provinces prior to the amalgamation of Laurentia.

deficiency such as remaining ambiguity in the demonstration of primary remanence or the quality/precision of available geochronologic constraints. Additional poles that were not given an ‘A’ or ‘B’ classification at the Nordic Workshops are referred to as not-rated (‘NR’). These additional poles are taken from the Paleomagia database (Veikkolainen et al., 2014). Many of these poles are quite valuable for reconstruction and should not be dismissed from being considered in paleogeographic reconstructions. However, there are ambiguities associated with many of such poles not given Nordic ‘A’ or ‘B’ ratings in terms of how well the nature of the remanence is constrained including its age. For example, there are rich data associated with intrusive lithologies of the Grenville Province that are the available paleomagnetic constraints for Laurentia at the Mesoproterozoic-Neoproterozoic boundary. However, the ages of the remanence associated with these poles is complicated by the reality that the magnetization was acquired during exhumation and such cooling ages are more difficult to robustly constrain than the ages of remanence associated with dated eruptive units or shallow-level intrusions. As a result, the vast majority of Grenville Province poles are not given an ‘A’ or ‘B’ rating with the exception of the ‘B’ rated pole from the ca. 1015 Ma Haliburton intrusions. However, while any one of these Grenville poles could be interpreted to suffer from temporal uncertainty, the overall preponderance of poles in a similar location at the time suggests that they need to be taken seriously within any paleogeographic reconstruction of Laurentia (although note an alternative view of an allochthonous origin discussed below). In this compilation, the poles of Brown and McEnroe (2012) from the Adirondack highlands are used wherein the magnetic mineralogy and associated relative ages of remanence are well-constrained (Table 2). Additional not-rated poles included in the present compilation is the new pole for the ca. 1144 Ma Ontario lamprophyre dykes (Piispa et al., 2018) that strengthens the position of Laurentia at the time and coincides with the position of the poles from the ca. 1140 Ma Abitibi dikes (Ernst and Buchan, 1993). This pole will likely receive an ‘A’ rating when assessed at the next Nordic paleomagnetism workshop. Poles from the Chuar Group as presented in Eyster et al. (2019) are also included.

²⁴⁸ 3.4 Differential motion before Laurentia amalgamation

²⁴⁹ Prior to the termination of the Trans-Hudson orogeny (before 1.8 Ga), paleomagnetic poles need
²⁵⁰ to be considered with respect to the individual Archean provinces. For the Superior province, an
²⁵¹ additional complexity is that paleomagnetic poles from Siderian to Rhyacian Period (2.50 to 2.05
²⁵² Ga) dike swarms, as well as deflection of dike trends, support an interpretation that there was
²⁵³ substantial Paleoproterozoic rotation of the western Superior province relative to the eastern
²⁵⁴ Superior province across the Kapuskasing Structural Zone (Bates and Halls, 1991; Evans and
²⁵⁵ Halls, 2010). This interpretation is consistent with the hypothesis of Hoffman (1988) that the
²⁵⁶ Kapuskasing Structural Zone represents major intracratonic uplift related to the Trans-Hudson
²⁵⁷ orogeny. Evans and Halls (2010) propose an Euler rotation of (51°N, 85°W, -14°CCW) to
²⁵⁸ reconstruct western Superior relative to eastern Superior and interpret that the rotation occurred
²⁵⁹ in the time interval of 2.07 to 1.87 Ga. I follow this interpretation and group the poles into
²⁶⁰ Superior (West) and Superior (East). Uncertainty remains with respect to whether the ca. 1.88
²⁶¹ Ga Molson dikes pole pre-dates or post-dates this rotation and thus for the time being should be
²⁶² considered solely in the western Superior province reference frame.

²⁶³ There are poles in the compilation for the Slave, Wyoming, Rae, Superior and Nain provinces
²⁶⁴ prior to Laurentia amalgamation (Fig. 3 and Table 2). Overall, these data provide an
²⁶⁵ opportunity to re-evaluate the paleomagnetic evidence for relative motions between Archean
²⁶⁶ provinces prior to Laurentia assembly. A lingering question raised in Hoffman (1988) that still
²⁶⁷ remains is to what extent the Archean provinces each had independent drift histories with
²⁶⁸ significant separation or shared histories before experiencing fragmentation and reamalgamation.
²⁶⁹ The strongest analysis in this regard comes from comparisons between paleomagnetic poles
²⁷⁰ between the Superior and Slave provinces (Buchan et al., 2009; Mitchell et al., 2014; Buchan
²⁷¹ et al., 2016). High-quality paleomagnetic poles from these two provinces provide strong support
²⁷² for differential motion between the Superior and Slave provinces between 2.2 and 1.8 Ga with the
²⁷³ two provinces not being in their relative orientation to one another either and having distinct pole
²⁷⁴ paths as constrained by 5 time periods of nearly coeval poles from 2.23 and 1.89 Ga (Fig. 4;
²⁷⁵ Buchan et al., 2016. These data provide paleomagnetic support for the Superior and Slave
²⁷⁶ provinces having independent histories of differential motion. They also support the hypothesis

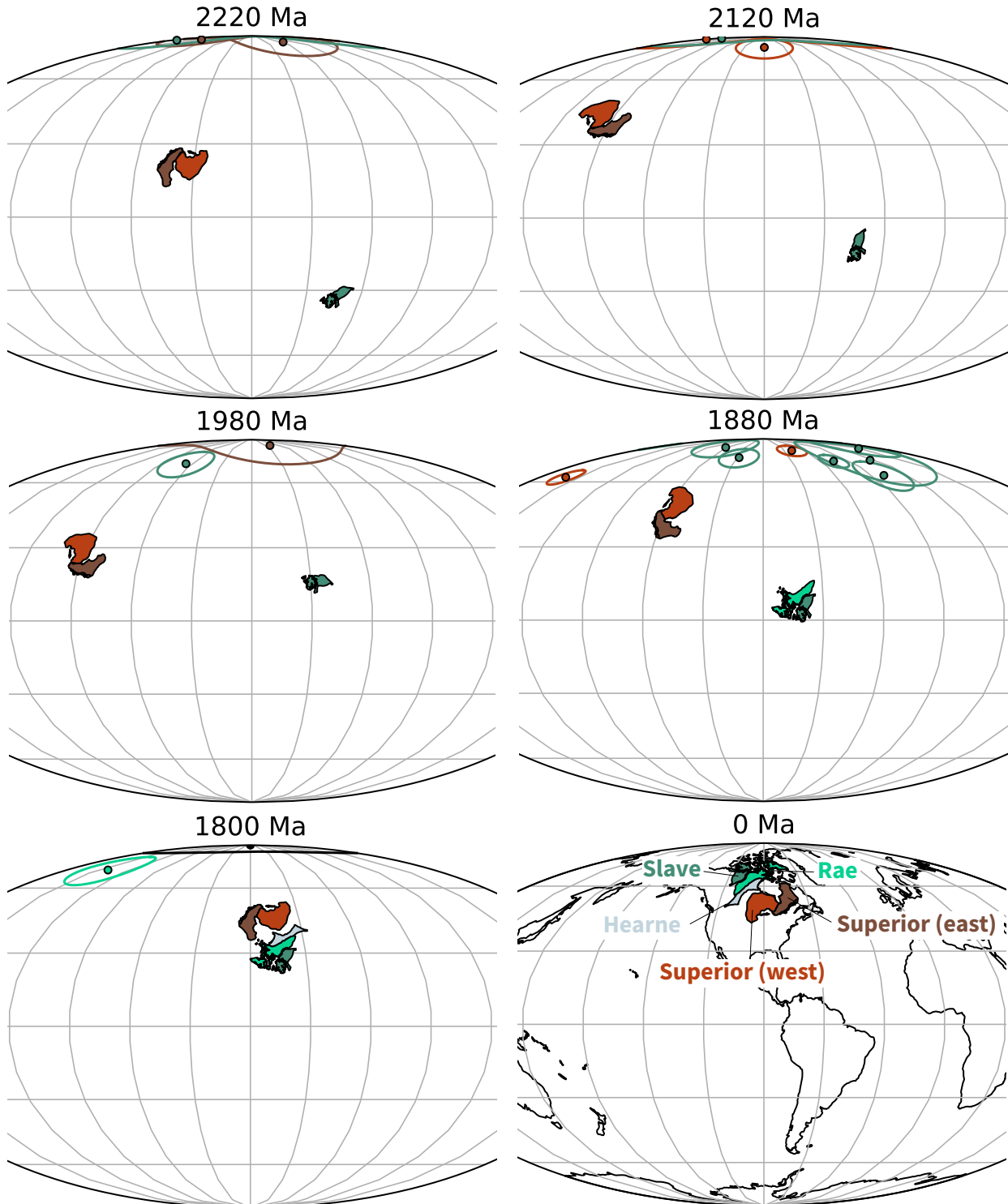


Figure 4. Paleogeographic reconstructions developed using poles from the Superior, Slave and Rae provinces. Paleomagnetic poles are shown colored to match their respective province with these provinces shown in present-day coordinates and labeled in the 0 Ma panel. Poles with ages that are within 25 million years of the given time slice are shown. The relatively well-resolved pole paths from the Superior and Slave provinces (Fig. 3) that are utilized for these reconstructions provide strong support for differential plate tectonic motion between 2220 and 1850 Ma.

277 that the Trans-Hudson orogeny is the result of terminal collision associated with the closure of an
278 ocean basin between the Superior province and the Hearne+Rae+Slave provinces.

279 Reconstructions developed for this chapter of the Superior and Slave provinces using these poles
280 are shown in Figure 4 and illustrate the difference in implied orientation and paleolatitude that
281 results from these well-constrained poles.

282 **3.5 Paleogeography of an assembled Laurentia**

283 Following the amalgamation of the Archean provinces in Laurentia ca. 1.8 Ga, poles from each
284 part of Laurentia can be considered to reflect the position of the entire composite craton. It is
285 worth considering the possibility that poles from zones of Paleoproterozoic and Mesoproterozoic
286 accretion could be allochthonous to the craton. Halls (2015) argued that this was the case for late
287 Mesoproterozoic and early Neoproterozoic poles from east of the Grenvillian allochthon boundary
288 fault. However, the majority of researchers have considered these poles to post-date major
289 differential motion and be associated with cooling during collapse of a thick orogenic plateau
290 developed during continent-continent collision (e.g. Brown and McEnroe, 2012). Poles with a
291 B-rating are also included in the composite that come from Greenland, Svalbard and Scotland.

292 These terranes were once part of contiguous Laurentia, but have subsequently rifted away. These
293 poles need to be rotated into the Laurentia reference frame prior to use for tectonic
294 reconstruction and I apply the rotations shown in Table 1. The Euler pole and rotation is quite
295 well-constrained for Greenland as it is associated with recent opening of Baffin Bay and the
296 Labrador Sea (for which the rotation of Roest and Srivastava, 1989 is used). The reconstruction
297 of Scotland is associated with the opening of the Atlantic (for which the rotation employed by
298 Torsvik and Cocks, 2017 is used) which is well-constrained but has more uncertainty associated
299 with the Euler pole than that for Greenland. The reconstruction of Svalbard is more challenging
300 given a multi-state tectonic history involving both translation within the Caledonides and
301 subsequent rifting. The preferred Euler of Maloof et al. (2006) is used here that designed, in
302 particular, to honor the high degree of similarity between Tonian sediments in East Greenland
303 (Hoffman et al., 2012) and those of East Svalbard (Maloof et al., 2006).

304 Through the Proterozoic, there are intervals where there are abundant paleomagnetic poles

305 that constrain Laurentia's position and intervals when the record is quite sparse (shown colored
306 by age in Fig. 3). To further visualize the temporal coverage of the poles and to summarize the
307 motion, implied paleolatitudes for an interior point on Laurentia are shown in Figure 5. The ages
308 of poles are also shown in comparison to the simplified summary of tectonic events in Figure 2.
309 Both collisional and extensional tectonism can result in the formation of lithologies that can be
310 used to develop paleomagnetic poles either as a result of basin formation, magmatism or both. In
311 addition, intraplate magmatism resulting from plume-related large-igneous provinces can lead to
312 paleomagnetic poles in periods that are otherwise characterized by tectonic quiescence (e.g. the
313 ca. 1267 Ma Mackenzie LIP; Fig. 2). Intracontinental rifts have led to the highest density of poles
314 both in the case of the ca. 1.4 Ga Belt Supergroup and the ca. 1.1 Ga Midcontinent Rift (Fig. 2).
315 The quality and resolution of the record from the Midcontinent Rift is aided by the voluminous
316 magmatism that occurred in conjunction with basin formations that enables the development of
317 well-calibrated apparent polar wander path (Swanson-Hysell et al., 2019). The late Tonian Period
318 also has a number of poles including the Gunbarrel LIP (ca. 780 Ma) and Franklin LIP (ca. 720
319 Ma), as well as similarly-aged sedimentary rocks from western Laurentia basins (Eyster et al.,
320 2019). Overall, the record of paleomagnetic poles has a lot of internal consistency in intervals for
321 which there is high-resolution coverage. These data result in the progressive paths agreement
322 between poles such as ascending up to the Logan Loop, down the Keweenawan Track
323 (Swanson-Hysell et al., 2019) to the Grenville Loop prior to a temporal gap before the late Tonian
324 (ca. 775 to 720 Ma) path (Eyster et al., 2019).

325 Data from other terranes add resolution to the record. In particular, data from Greenland
326 adds 12 poles between 1385 and 1160 Ma when there are only 4 poles from mainland Laurentia.
327 Given that the rotation between Greenland and mainland Laurentia is well-constrained (Table 1),
328 once rotated these poles can be used for reconstruction of the entire continent. The reliability of
329 this approach gains credence through the good agreement between the ca. 1633 Ma Melville Bugt
330 diabase dykes pole from Greenland (Halls et al., 2011) and the ca. 1590 Ma Western Channel
331 diabase pole of mainland Laurentia (Irving and Park, 1972). Similarly, there is good agreement
332 between the ca. 1267 Ma Mackenzie dykes pole of Laurentia (Buchan et al., 2000) and coeval
333 poles from Greenland such as the ca. 1275 Ma North Qoroq intrusives (Piper, 1992) and Kungnat

³³⁴ Ring dyke (Piper, 1977). Furthermore, the Greenland poles with ages that fall between the ca.
³³⁵ 1237 Ma Sudbury dikes and ca. 1143 Ma lamprophyre dykes pole of mainland Laurentia are
³³⁶ consistent with constraints on either side from the mainland while filling in the ascending limb of
³³⁷ the path leading up to the apex of 1140 to 1108 Ma poles known as the Logan Loop (Fig. ??).

³³⁸ An exception to this overall agreement between poles from Greenland and mainland Laurentia
³³⁹ occurs ca. 1382 Ma. There are poles of this age from Greenland associated with the Zig-Zag Dal
³⁴⁰ basalts and related intrusions (Marcussen and Abrahamsen, 1983; Abrahamsen and Van Der Voo,
³⁴¹ 1987). However, these poles are in a distinct location from poles of similar age associated with the
³⁴² Belt Supergroup (e.g. the McNamara Formation and Pilcher/Garnet Range and Libby
³⁴³ Formations; Elston et al., 2002). Additionally, the older Belt Supergroup poles form a more
³⁴⁴ southerly population than time-equivalent poles from elsewhere in Laurentia such as the Mistastin
³⁴⁵ Pluton. There are potential complications associated with the Belt Supergroup being exposed
³⁴⁶ within thrust sheets with significant Cenozoic Mesozoic and Cenozoic deformation. However,
³⁴⁷ vertical axis rotations of the Belt region are not able to bring the Belt poles into agreement with
³⁴⁸ those from Laurentia or Greenland nor is translation away from the craton. Another potential
³⁴⁹ complication is that the remanence used for the development of the Belt Supergroup resides in
³⁵⁰ hematite. As a result, there is the potential for inclination-flattening within the sedimentary rocks
³⁵¹ from which poles are developed. However, applying a moderate inclination factor of $f = 0.6$ also
³⁵² does not bring the poles into congruence with the Zig-Zag basalts. There is the potential that the
³⁵³ hematite could be the result of post-depositional oxidation (the remanence of the Purcell lavas
³⁵⁴ pole is also held by hematite) however the overall coherency of the pole directions and the
³⁵⁵ presence of reversals has been taken as evidence that the remanence is primary (Elston et al.,
³⁵⁶ 2002). At present, it is unclear which poles are a better representation of Laurentia's position ca.
³⁵⁷ 1400 Ma.

³⁵⁸ Another challenging portion of the Laurentia record is that for the Ediacaran Period where
³⁵⁹ there is little consistency between poles of similar age (Figs. 3 and ??). As a result, there are
³⁶⁰ poles that imply both low-latitude and high-latitude positions of Laurentia between 615 and 565
³⁶¹ Ma. One explanation for these variable pole positions is that they are the result of large-scale
³⁶² oscillatory true polar wander in the Ediacaran that has influenced poles in Baltica and West

363 Africa as well (McCausland et al., 2007; Robert et al., 2017). Another possibility is that the lack
364 of congruency between poles in this point in the record is due to a particularly weak and
365 non-dipolar geomagnetic field (Abrajevitch and Van der Voo, 2010; Bono et al., 2019). Regardless
366 of mechanism, the Ediacaran data stand out as anomalous relative to the coherency of the rest of
367 the poles in the composite (Fig. 5).

368 Synthesizing the compilation of paleomagnetic poles for Laurentia into a composite path over
369 the past 1.8 billion years presents a challenge given the highly variable temporal coverage. The
370 method typically applied in the Phanerozoic is to develop synthesized pole paths either through
371 fitting spherical splines through the data or calculating binned running means where the Fisher
372 mean of poles within a given interval are calculated (Torsvik et al., 2012). Applying such an
373 approach can reduce the effect of spurious poles in regions of high data density where seeking to
374 satisfy every mean pole position would result in jerky motion.

375 A synthesized pole path for Laurentia is developed here and used to develop a continuous
376 paleogeographic reconstruction of Laurentia constrained by the compilation of paleomagnetic
377 poles. The paleolatitude implied by this continuous model is shown in Figure 5. This path is
378 based on Laurentia data alone which means that it is poorly constrained through intervals of
379 sparse data (950-850 Ma for example). One could use interpretations of paleogeographic
380 connections with other cratons (e.g. Baltica in the early Neoproterozoic) to fill in such portions of
381 the path, however the result then becomes model-dependent without being constrained by data
382 from Laurentia itself. In portions of the record with a more dense record of poles, such as ca.
383 1450, a calculated running mean is used to integrate constraints from multiple poles. This
384 method follows the approach taken in the Phanerozoic (e.g. Torsvik et al., 2012 wherein all poles
385 within a 20 Myr interval are averaged with the interval than progressively moved forward in 10
386 Myr steps. When there are isolated ‘A’ grade poles without other temporally-similar poles, these
387 poles are fully satisfied in model. Where there are no constraints a simple interpolation between
388 constraints is made. While data from Scotland and Svalbard are associated with Laurentia, the
389 Scotland poles are poorly constrained in time and the Svalbard rotation to Laurentia is uncertain.
390 These poles are not utilized in the simple Laurentia model which means that the model as shown
391 does not include oscillatory true polar wander interpreted to have occurred ca. 810 and 790 Ma

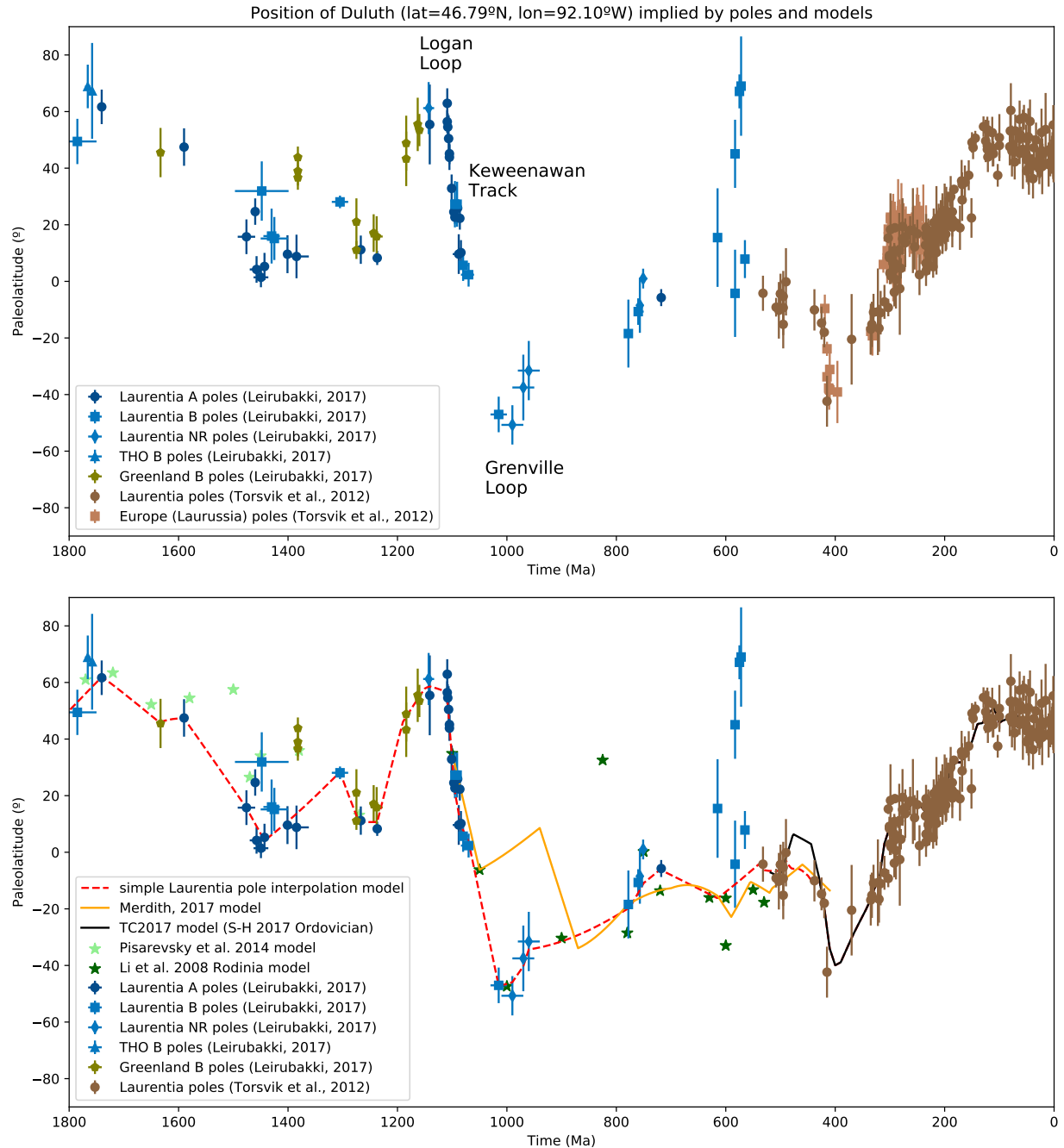


Figure 5. Top panel: Paleolatitude implied by paleomagnetic poles from Laurentia and associated blocks for Duluth (lat=46.79°N, lon=92.10°W). The paleomagnetic poles are compiled in Table 2. Bottom panel: Paleolatitude implied by Laurentia poles compared with that implied by published paleogeographic models and the simple Laurentia model used in this chapter for the reconstructions in Figure 6.

³⁹² based on data from Svalbard (Maloof et al., 2006).

³⁹³ One downside of a running mean approach is that it pulls the mean to regions of high data
³⁹⁴ density. As was shown in Swanson-Hysell et al. (2019), this behavior can reduce motion along an
³⁹⁵ apparent polar wander path. As a result, for the portion of the reconstruction during the interval
³⁹⁶ of time ca. 1110 to 1070 Ma, I utilize an Euler pole inversion from Swanson-Hysell et al. (2019).

³⁹⁷ Paleogeographic snapshots for the past position of Laurentia reconstructed using this synthesis
³⁹⁸ of the paleomagnetic poles are shown in Figure 6. These reconstructions use the tectonic elements
³⁹⁹ as defined by Whitmeyer and Karlstrom (2007) with these elements being progressively added
⁴⁰⁰ associated with Laurentia's accretionary growth. As a reminder to the reader, paleomagnetic
⁴⁰¹ poles provide constraints on the paleolatitude of a continental block as well as its orientation
⁴⁰² (which way was north relative to the block). While they provide constraints in this regard, they
⁴⁰³ do not provide constraints in and of themselves of the longitudinal position of the block. Other
⁴⁰⁴ approaches to obtain paleolongitude utilize geophysical hypotheses such as assuming that large
⁴⁰⁵ low shear velocity provinces have been stable plume-generating zones in the lower mantle to
⁴⁰⁶ which plumes can be reconstructed (Torsvik et al., 2014) or that significant pole motion in certain
⁴⁰⁷ time intervals is associated with true polar wander axes that switch through time in conjunction
⁴⁰⁸ with the supercontinent cycle (Mitchell et al., 2012). In Figure 6, Laurentia is centered on the
⁴⁰⁹ longitudinal position of Duluth with the orientation and paleolatitude being constrained by the
⁴¹⁰ paleomagnetic pole compilation as synthesized in the simple Laurentia pole interpolation model.
⁴¹¹ The continuous paleolatitude implied by this model is shown as the simple Laurentia pole
⁴¹² interpolation mode in Figure 5.

⁴¹³ 3.6 Comparing paleogeographic models to the paleomagnetic compilation

⁴¹⁴ Developing comprehensive global continuous paleogeographic models is a major challenge given
⁴¹⁵ the need to integrate and satisfy diverse geological and paleomagnetic data types. Continually
⁴¹⁶ improving constraints related to tectonic setting from improved geologic and geochronologic data
⁴¹⁷ need to be carefully integrated with the database of paleomagnetic poles. Paleomagnetic poles
⁴¹⁸ compilations themselves are evolving with better data and improved geochronology. Efforts such

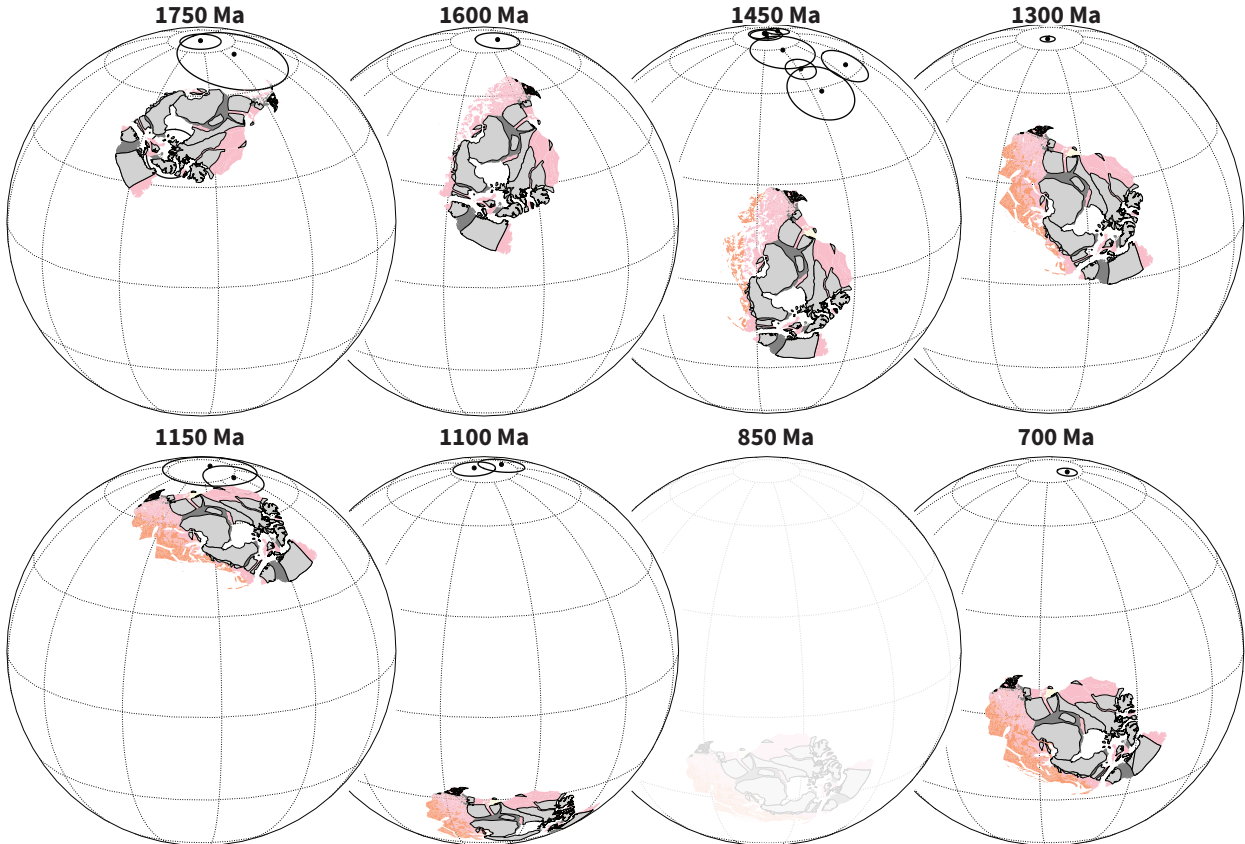


Figure 6. Paleogeographic reconstructions of Laurentia at time intervals through the Proterozoic that are well-constrained by paleomagnetic data. These reconstructions use the simple Laurentia pole interpolation model that is shown in Figure 5 and use this model to reconstruct the tectonic elements of Whitmeyer and Karlstrom (2007) shown in Figure 1. Modern coastlines are maintained in these polygons so that the rotated orientations can be interpreted by the reader in comparison to Figure 1. Paleomagnetic poles within 25 million years of each reconstruction time are plotted. All reconstructions have poles within such a time frame that provide constraints with the exception of the 850 Ma reconstruction which is shown faintly given this relative uncertainty in Laurentia's position.

419 as this volume are therefore essential to present the state-of-the-art in terms of existing
 420 constraints that can be used to evaluate current models and set the stage for future progress in
 421 Precambrian paleogeography.

422 There is an overall lack of published continuous models in the literature for the Proterozoic
 423 that can be compared to the compilation of paleomagnetic poles presented herein. The approach
 424 in the community for many years has been to publish models as snapshots at given time intervals
 425 presented in figures without publishing continuous rotation parameters. With the further
 426 adoption of software tools such as GPlates, there has been significant progress in the publication
 427 of continuous paleogeographic models constrained by paleomagnetic poles through the

⁴²⁸ Phanerozoic (540 Ma to present; e.g. Torsvik et al., 2012).

⁴²⁹ An exception to the paucity of published continuous paleogeographic models for the
⁴³⁰ Precambrian is the Neoproterozoic model of Merdith et al. (2017) which is shown in comparison
⁴³¹ to the constraints for Laurentia in Figure 5. The extent to which the implied position of
⁴³² Laurentia in Merdith et al. (2017) is consistent with the compiled paleomagnetic constraints can
⁴³³ be visualized in Figure 5. As noted above, the development of such models is challenging and the
⁴³⁴ researchers need to balance varying constraints. The focus here will be on the extent to which
⁴³⁵ this model satisfies the available paleomagnetic poles for Laurentia. The model does not honor
⁴³⁶ the Grenville loop (e.g. go to moderately high southerly latitudes ca. 1000 Ma) which is a striking
⁴³⁷ departure from the paleomagnetic record and standard paleogeographic models. Additionally, the
⁴³⁸ implemented plate motion strays from the younger poles of the Keweenawan Track and does not
⁴³⁹ honor the Franklin LIP pole Denyszyn et al. (2009b) despite its ‘A’ Nordic rating. The Franklin
⁴⁴⁰ pole is taken to be a key constraint at the Tonian/Cryogenian boundary that provides evidence of
⁴⁴¹ the supercontinent Rodinia being equatorial and for the Sturtian glaciation having extended to
⁴⁴² equatorial latitudes (Macdonald et al., 2010).

⁴⁴³ There are more published models that show snapshots and publish rotation parameters
⁴⁴⁴ associated with given time intervals such as the Rodinia model of Li et al. (2008) and the
⁴⁴⁵ Mesoproterozoic model of Pisarevsky et al. (2014), but did not publish parameters for a
⁴⁴⁶ continuous model. The position for Laurentia implied by the Euler poles given for the model
⁴⁴⁷ snapshots of these studies are shown in Figure 5 and can be compared to the compiled record.

⁴⁴⁸ 3.7 Conclusion

⁴⁴⁹ There is strong evidence both in Laurentia’s geological and paleomagnetic record for differential
⁴⁵⁰ plate tectonic motion between 2.2 and 1.8 Ga. The continued history of accretionary orogenesis
⁴⁵¹ and the evaluation of Laurentia’s pole path in comparison to other continents from 1.8 Ga onward
⁴⁵² supports the continual operation of plate tectonics throughout the rest of the Proterozoic and
⁴⁵³ Phanerozoic as well. While this evidence fits with the majority of interpretations of the timing of
⁴⁵⁴ initiation of modern-style plate tectonics (see summary in Korenaga, 2013), there continue to be

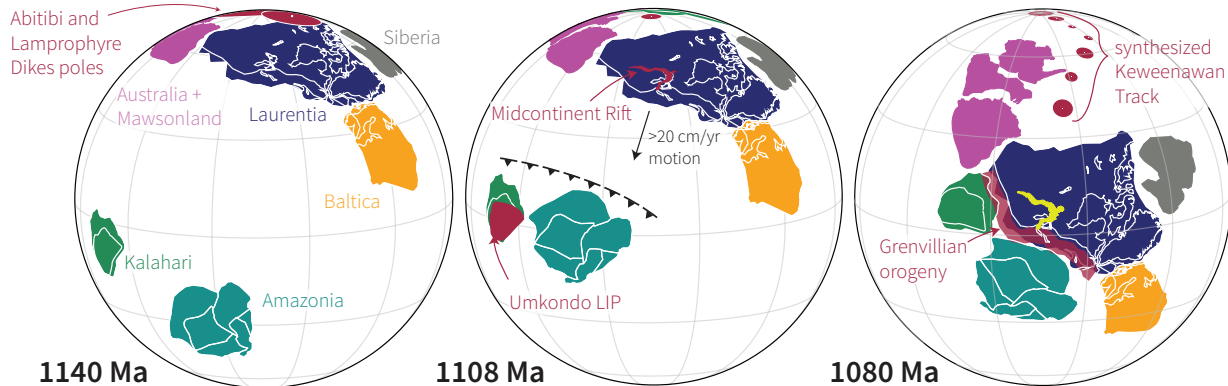


Figure 7. Paleogeographic reconstructions of Laurentia and other select Proterozoic continents leading up to Rodinia assembly in the late Mesoproterozoic modified from Swanson-Hysell et al. (2019). The record of paleomagnetic poles implies rapid motion which is consistent with the timing of collisional orogenesis associated with the Grenvillian orogeny.

455 arguments proposing that a stagnant lid persisted through the Mesoproterozoic Era (1.6 to 1.0
 456 Ga) and into the Neoproterozoic with plate tectonics not initiating until ca. 0.8 Ga (Hamilton,
 457 2011; Stern and Miller, 2018). These arguments rest largely on the relative lack of the types of
 458 low-temperature high-pressure metamorphic rocks such as blueschists that form in subduction
 459 zones in the Proterozoic relative to the Phanerozoic (Stern et al., 2013). An alternative
 460 interpretation for this lack of blueschists in the Proterozoic is that such a shift in metamorphic
 461 regime is the predicted result of secular evolution of mantle chemistry rather than a harbinger of
 462 the onset of plate tectonics (Palin and White, 2015). While this line of evidence is intriguing, to
 463 argue that there was not differential plate tectonic motion in the Paleoproterozoic and
 464 Mesoproterozoic is to ignore a vast breadth and depth of geological and paleomagnetic data. As
 465 an example, consider the record of Laurentia in the late Mesoproterozoic. As can be seen in Table
 466 2, there are many high-quality paleomagnetic poles between 1110 and 1070 Ma. These poles
 467 constrain rapid motion of Laurentia leading up to collisional orogenesis as illustrated in Figure 7
 468 providing strong evidence for differential plate motion at the time.

469 The paleogeographic record of Laurentia is rich in constraints through the Precambrian both
 470 in terms of the geological and geochronological constraints on tectonism and the record of
 471 paleomagnetic poles. As can be seen in the Chapters on Archean paleogeography (Salminen et al.,
 472 this volume), Nuna (Elming et al., this volume) and Rodinia (Evans et al., this volume), these
 473 constraints are at the center of developing paleogeographic models through the Precambrian and

⁴⁷⁴ will continue to be moving forward.

⁴⁷⁵ Acknowledgements

⁴⁷⁶ Many participants in the Nordic Paleomagnetism Workshop have contributed to the compilation
⁴⁷⁷ and evaluation of the pole list utilized herein. Particular acknowledgement goes to David Evans
⁴⁷⁸ for maintaining and distributing the compiled pole lists as well as additional efforts of Lauri
⁴⁷⁹ Pesonen in maintaining the Paleomagia database (Veikkolainen et al., 2014). GPlates, and in
⁴⁸⁰ particular the pyGPlates API, was utilized in this work (Müller et al., 2018). Figures were made
⁴⁸¹ using Matplotlib (Hunter, 2007) in conjunction with cartopy (Met Office, 2010 - 2015) and
⁴⁸² pmagpy (Tauxe et al., 2016) within an interactive Python environment (Pérez and Granger,
⁴⁸³ 2007). This work was supported by NSF CAREER Grant EAR-1847277 awarded to N.L.S.-H.
⁴⁸⁴ The code, data, and reconstructions used in this paper are openly available in this repository:
⁴⁸⁵ https://github.com/Swanson-Hysell-Group/Laurentia_Paleogeography.

⁴⁸⁶ References

- ⁴⁸⁷ Abrahamsen, N. and Van Der Voo, R., 1987, Palaeomagnetism of middle Proterozoic (c. 1.25 Ga) dykes from central
⁴⁸⁸ North Greenland: Geophysical Journal International, v. 91, p. 597–611, doi:10.1111/j.1365-246x.1987.tb01660.x.
- ⁴⁸⁹ Abrajevitch, A. and Van der Voo, R., 2010, Incompatible Ediacaran paleomagnetic directions suggest an equatorial
⁴⁹⁰ geomagnetic dipole hypothesis: Earth and Planetary Science Letters, v. 293, p. 164–170.
- ⁴⁹¹ Bates, M. P. and Halls, H. C., 1991, Broad-scale Proterozoic deformation of the central Superior Province revealed
⁴⁹² by paleomagnetism of the 2.45 Ga Matachewan dyke swarm: Canadian Journal of Earth Sciences, v. 28, p.
⁴⁹³ 1780–1796, doi:10.1139/e91-159.
- ⁴⁹⁴ Berman, R., Davis, A., and Pehrsson, S., 2007, Collisional Snowbird tectonic zone resurrected: Growth of Laurentia
⁴⁹⁵ during the 1.9 Ga accretionary phase of the Hudsonian orogeny: Geology, v. 35, p. 911–914,
⁴⁹⁶ doi:10.1130/G23771A.1.
- ⁴⁹⁷ Bickford, M., Van Schmus, W., Karlstrom, K., Mueller, P., and Kamenov, G., 2015,
⁴⁹⁸ Mesoproterozoic-trans-Laurentian magmatism: A synthesis of continent-wide age distributions, new SIMS U–Pb
⁴⁹⁹ ages, zircon saturation temperatures, and Hf and Nd isotopic compositions: Precambrian Research, v. 265, p.
⁵⁰⁰ 286–312, doi:10.1016/j.precamres.2014.11.024.

- 501 Bond, G., Nickleson, P., and Kominz, M., 1984, Breakup of a supercontinent between 625 and 555 Ma: new
502 evidence and implications for continental histories: *Earth and Planetary Science Letters*, v. 70, p. 325–345,
503 doi:10.1016/0012-821X(84)90017-7.
- 504 Bono, R. K., Tarduno, J. A., Nimmo, F., and Cottrell, R. D., 2019, Young inner core inferred from Ediacaran
505 ultra-low geomagnetic field intensity: *Nature Geoscience*, v. 12, p. 143–147, doi:10.1038/s41561-018-0288-0.
- 506 Books, K., 1972, Paleomagnetism of some Lake Superior Keweenawan rocks: U.S. Geological Survey Professional
507 Paper, v. P 0760, p. 42.
- 508 Borradaile, G. and Middleton, R., 2006, Proterozoic paleomagnetism in the Nipigon Embayment of northern
509 Ontario: Pillar Lake Lava, Waweig Troctolite and Gunflint Formation tuffs: *Precambrian Research*, v. 144, p.
510 69–91, doi:10.1016/j.precamres.2005.10.007.
- 511 Brown, L. L. and McEnroe, S. A., 2012, Paleomagnetism and magnetic mineralogy of Grenville metamorphic and
512 igneous rocks, Adirondack Highlands, USA: *Precambrian Research*, v. 212–213, p. 57–74,
513 doi:10.1016/j.precamres.2012.04.012.
- 514 Buchan, K., Mertanen, S., Park, R., Pesonen, L., Elming, S. A., Abrahamsen, N., and Bylund, G., 2000, Comparing
515 the drift of Laurentia and Baltica in the Proterozoic: the importance of key paleomagnetic poles:
516 *Tectonophysics*, v. 319, p. 167–198.
- 517 Buchan, K. L., LeCheminant, A. N., and van Breemen, O., 2009, Paleomagnetism and U–Pb geochronology of the
518 Lac de Gras diabase dyke swarm, Slave Province, Canada: implications for relative drift of Slave and Superior
519 provinces in the Paleoproterozoic: *Canadian Journal of Earth Sciences*, v. 46, p. 361–379, doi:10.1139/e09-026.
- 520 Buchan, K. L., LeCheminant, A. N., and van Breemen, O., 2012, Malley diabase dykes of the Slave craton,
521 Canadian Shield: U–Pb age, paleomagnetism, and implications for continental reconstructions in the early
522 Paleoproterozoic: *Canadian Journal of Earth Sciences*, v. 49, p. 435–454, doi:10.1139/e11-061.
- 523 Buchan, K. L., Mitchell, R. N., Bleeker, W., Hamilton, M. A., and LeCheminant, A. N., 2016, Paleomagnetism of
524 ca. 2.13–2.11 Ga Indin and ca. 1.885 Ga Ghost dyke swarms of the Slave craton: Implications for the Slave
525 craton APW path and relative drift of Slave, Superior and Siberian cratons in the Paleoproterozoic: *Precambrian
526 Research*, v. 275, p. 151–175, doi:10.1016/j.precamres.2016.01.012.
- 527 Buchan, K. L., Mortensen, J. K., and Card, K. D., 1993, Northeast-trending early Proterozoic dykes of southern
528 Superior Province: multiple episodes of emplacement recognized from integrated paleomagnetism and U–Pb
529 geochronology: *Canadian Journal of Earth Sciences*, v. 30, p. 1286–1296, doi:10.1139/e93-110.
- 530 Burton, W. C. and Southworth, S., 2010, A model for Iapetan rifting of Laurentia based on Neoproterozoic dikes
531 and related rocks: From Rodinia to Pangea: The Lithotectonic Record of the Appalachian Region, p. 455–476,
532 doi:10.1130/2010.1206(20).

- 533 Casquet, C., Dahlquist, J. A., Verdecchia, S. O., Baldo, E. G., Galindo, C., Rapela, C. W., Pankhurst, R. J.,
534 Morales, M. M., Murra, J. A., and Mark Fanning, C., 2018, Review of the Cambrian Pampean orogeny of
535 Argentina; a displaced orogen formerly attached to the Saldania Belt of South Africa?: *Earth-Science Reviews*, v.
536 177, p. 209–225, doi:10.1016/j.earscirev.2017.11.013.
- 537 Condit, C. B., Mahan, K. H., Ault, A. K., and Flowers, R. M., 2015, Foreland-directed propagation of high-grade
538 tectonism in the deep roots of a Paleoproterozoic collisional orogen, SW Montana, USA: *Lithosphere*, p. L460.1,
539 doi:10.1130/l460.1.
- 540 Corrigan, D., Pehrsson, S., Wodicka, N., and de Kemp, E., 2009, The Palaeoproterozoic Trans-Hudson Orogen: a
541 prototype of modern accretionary processes: Geological Society, London, Special Publications, v. 327, p. 457–479,
542 doi:10.1144/sp327.19.
- 543 Dahl, P. S., Holm, D. K., Gardner, E. T., Hubacher, F. A., and Foland, K. A., 1999, New constraints on the timing
544 of Early Proterozoic tectonism in the Black Hills (South Dakota), with implications for docking of the Wyoming
545 province with Laurentia: *Geological Society of America Bulletin*, v. 111, p. 1335–1349,
546 doi:10.1130/0016-7606(1999)111<1335:ncotto>2.3.co;2.
- 547 Denyszyn, S. W., Davis, D. W., and Halls, H. C., 2009a, Paleomagnetism and U–Pb geochronology of the Clarence
548 Head dykes, Arctic Canada: orthogonal emplacement of mafic dykes in a large igneous province: *Canadian
549 Journal of Earth Sciences*, v. 46, p. 155–167, doi:10.1139/E09-011.
- 550 Denyszyn, S. W., Halls, H. C., Davis, D. W., and Evans, D. A. D., 2009b, Paleomagnetism and U–Pb geochronology
551 of Franklin dykes in High Arctic Canada and Greenland: a revised age and paleomagnetic pole constraining block
552 rotations in the Nares Strait region: *Canadian Journal of Earth Sciences*, v. 46, p. 689–705, doi:10.1139/E09-042.
- 553 Dickerson, P. W. and Keller, M., 1998, The Argentine Precordillera: its odyssey from the Laurentian Ouachita
554 margin towards the Sierras Pampeanas of Gondwana: Geological Society, London, Special Publications, v. 142,
555 p. 85–105, doi:10.1144/gsl.sp.1998.142.01.05.
- 556 Donadini, F., Pesonen, L. J., Korhonen, K., Deutsch, A., and Harlan, S. S., 2011, Paleomagnetism and
557 paleointensity of the 1.1 Ga old diabase sheets from central Arizona: *Geophysica*, v. 47, p. 3–30.
- 558 Elming, S. Å., D’Agrella-Filho, M. S., Page, L. M., Tohver, E., Trindade, R. I. F., Pacca, I. I. G., Geraldes, M. C.,
559 and Teixeira, W., 2009, A palaeomagnetic and 40Ar/39Ar study of late precambrian sills in the SW part of the
560 Amazonian craton: Amazonia in the Rodinia reconstruction: *Geophysical Journal International*, v. 178, p.
561 106–122.
- 562 Elston, D. P., Enkin, R. J., Baker, J., and Kisilevsky, D. K., 2002, Tightening the Belt: Paleomagnetic-stratigraphic
563 constraints on deposition, correlation, and deformation of the Middle Proterozoic (ca. 1.4 Ga) Belt-Purcell
564 Supergroup, United States and Canada: *GSA Bulletin*, v. 114, p. 619–638,
565 doi:10.1130/0016-7606(2002)114<619:TTBPSC>2.0.CO;2.

- 566 Emslie, R. F., Irving, E., and Park, J. K., 1976, Further paleomagnetic results from the Michikamau Intrusion,
567 Labrador: Canadian Journal of Earth Sciences, v. 13, p. 1052–1057, doi:10.1139/e76-108.
- 568 Ernst, R. and Buchan, K., 1993, Paleomagnetism of the Abitibi dike swarm, southern Superior Province, and
569 implications for the Logan Loop: Canadian Journal of Earth Science, v. 30, p. 1886–1897, doi:10.1139/e93-167.
- 570 Evans, D. and Halls, H., 2010, Restoring Proterozoic deformation within the Superior craton: Precambrian
571 Research, v. 183, p. 474 – 489, doi:10.1016/j.precamres.2010.02.007.
- 572 Evans, M. E. and Bingham, D. K., 1973, Paleomagnetism of the Precambrian Martin Formation, Saskatchewan:
573 Canadian Journal of Earth Sciences, v. 10, p. 1485–1493, doi:10.1139/e73-141.
- 574 Evans, M. E. and Hoye, G. S., 1981, Paleomagnetic results from the lower proterozoic rocks of Great Slave Lake and
575 Bathurst Inlet areas, Northwest Territories: *In* Proterozoic Basins of Canada; Geological Survey of Canada,
576 Paper 81-10, Natural Resources Canada/ESS/Scientific and Technical Publishing Services, doi:10.4095/109374.
- 577 Eyster, A., Weiss, B. P., Karlstrom, K., and Macdonald, F. A., 2019, Paleomagnetism of the Chuar Group and
578 evaluation of the late Tonian Laurentian apparent polar wander path with implications for the makeup and
579 breakup of Rodinia: GSA Bulletin, doi:10.1130/b32012.1.
- 580 Fahrig, W. and Bridgwater, D., 1976, Late Archean-early Proterozoic paleomagnetic pole positions from west
581 Greenland: *In* Windley, B., ed., Early History of the Earth, Wiley, p. 427–442.
- 582 Fahrig, W. F. and Jones, D. L., 1976, The paleomagnetism of the Helikian Mistastin pluton, Labrador, Canada:
583 Canadian Journal of Earth Sciences, v. 13, p. 832–837, doi:10.1139/e76-086.
- 584 Fairchild, L. M., Swanson-Hysell, N. L., Ramezani, J., Sprain, C. J., and Bowring, S. A., 2017, The end of
585 Midcontinent Rift magmatism and the paleogeography of Laurentia: Lithosphere, v. 9, p. 117–133,
586 doi:10.1130/L580.1.
- 587 Gala, M. G., Symons, D. T. A., and Palmer, H. C., 1995, Paleomagnetism of the Jan Lake Granite, Trans-Hudson
588 Orogen: Saskatchewan Geological Survey Summary of Investigations, v. 95-4.
- 589 Halls, H., 1974, A paleomagnetic reversal in the Osler Volcanic Group, northern Lake Superior: Canadian Journal
590 of Earth Science, v. 11, p. 1200–1207, doi:10.1139/e74-113.
- 591 Halls, H. C., 2015, Paleomagnetic evidence for ~4000 km of crustal shortening across the 1 Ga Grenville orogen of
592 North America: Geology, v. 43, p. 1051–1054, doi:10.1130/G37188.1.
- 593 Halls, H. C., Davis, D. W., Stott, G. M., Ernst, R. E., and Hamilton, M. A., 2008, The Paleoproterozoic Marathon
594 Large Igneous Province: New evidence for a 2.1 Ga long-lived mantle plume event along the southern margin of
595 the North American Superior Province: Precambrian Research, v. 162, p. 327–353,
596 doi:10.1016/j.precamres.2007.10.009.

- 597 Halls, H. C., Hamilton, M. A., and Denyszyn, S. W., 2011, The Melville Bugt Dyke Swarm of Greenland: A
598 Connection to the 1.5-1.6 Ga Fennoscandian Rapakivi Granite Province?, Springer Berlin Heidelberg, p. 509–535:
599 doi:10.1007/978-3-642-12496-9{_}27.
- 600 Halls, H. C. and Hanes, J. A., 1999, Paleomagnetism, anisotropy of magnetic susceptibility, and argon–argon
601 geochronology of the Clearwater anorthosite, Saskatchewan, Canada: Tectonophysics, v. 312, p. 235–248,
602 doi:10.1016/s0040-1951(99)00166-3.
- 603 Halverson, G. P., Porter, S. M., and Gibson, T. M., 2018, Dating the late Proterozoic stratigraphic record:
604 Emerging Topics in Life Sciences, v. 2, p. 137–147, doi:10.1042/etls20170167.
- 605 Hamilton, W. B., 2011, Plate tectonics began in Neoproterozoic time, and plumes from deep mantle have never
606 operated: Lithos, v. 123, p. 1–20, doi:10.1016/j.lithos.2010.12.007.
- 607 Harlan, S., 1993, Paleomagnetism of Middle Proterozoic diabase sheets from central Arizona: Canadian Journal of
608 Earth Science, v. 30, p. 1415–1426.
- 609 Harlan, S., Geissman, J., and Snee, L., 1997, Paleomagnetic and $^{40}\text{Ar}/^{39}\text{Ar}$ geochronologic data from late
610 Proterozoic mafic dykes and sills, Montana and Wyoming: USGS Professional Paper, v. 1580, p. 16.
- 611 Harlan, S. S. and Geissman, J. W., 1998, Paleomagnetism of the middle Proterozoic Electra Lake Gabbro, Needle
612 Mountains, southwestern Colorado: Journal of Geophysical Research: Solid Earth, v. 103, p. 15,497–15,507,
613 doi:10.1029/98jb01350.
- 614 Harlan, S. S., Geissman, J. W., and Snee, L. W., 2008, Paleomagnetism of Proterozoic mafic dikes from the Tobacco
615 Root Mountains, southwest Montana: Precambrian Research, v. 163, p. 239–264.
- 616 Harlan, S. S., Snee, L. W., Geissman, J. W., and Brearley, A. J., 1994, Paleomagnetism of the middle proterozoic
617 laramie anorthosite complex and sherman granite, southern laramie range, wyoming and colorado: Journal of
618 Geophysical Research: Solid Earth, v. 99, p. 17,997–18,020, doi:10.1029/94jb00580.
- 619 Henry, S., Mauk, F., and Van der Voo, R., 1977, Paleomagnetism of the upper Keweenawan sediments: Nonesuch
620 Shale and Freda Sandstone: Canadian Journal of Earth Science, v. 14, p. 1128–1138, doi:10.1139/e77-103.
- 621 Hildebrand, R. S., Hoffman, P. F., and Bowring, S. A., 2009, The Calderian orogeny in Wopmay orogen (1.9 Ga),
622 northwestern Canadian Shield: Geological Society of America Bulletin, v. 122, p. 794–814, doi:10.1130/B26521.1.
- 623 Hnat, J. S., van der Pluijm, B. A., and Van der Voo, R., 2006, Primary curvature in the Mid-Continent Rift:
624 Paleomagnetism of the Portage Lake Volcanics (northern Michigan, USA): Tectonophysics, v. 425, p. 71–82,
625 doi:10.1016/j.tecto.2006.07.006.
- 626 Hoffman, P., 1991, Did the breakout of Laurentia turn Gondwana inside out?: Science, v. 252, p. 1409–1412.

- 627 Hoffman, P. F., 1988, United plates of America, the birth of a craton: Early Proterozoic assembly and growth of
628 Laurentia: *Annual Review of Earth and Planetary Sciences*, v. 16, p. 543–603,
629 doi:10.1146/annurev.ea.16.050188.002551.
- 630 Hoffman, P. F., 1989, Speculations on Laurentia's first gigayear (2.0 to 1.0 Ga): *Geology*, v. 17, p. 135–138,
631 doi:10.1130/0091-7613(1989)017<0135:SOLSGF>2.3.CO;2.
- 632 Hoffman, P. F., Halverson, G. P., Domack, E. W., Maloof, A. C., Swanson-Hysell, N. L., and Cox, G. M., 2012,
633 Cryogenian glaciations on the southern tropical paleomargin of Laurentia (NE Svalbard and East Greenland),
634 and a primary origin for the upper Russøya (Islay) carbon isotope excursion: *Precambrian Research*, v. 206–207,
635 p. 137–158, doi:10.1016/j.precamres.2012.02.018.
- 636 Holm, D. K., Van Schmus, W. R., MacNeill, L. C., Boerboom, T. J., Schweitzer, D., and Schneider, D., 2005, U-Pb
637 zircon geochronology of Paleoproterozoic plutons from the northern midcontinent, USA: Evidence for subduction
638 flip and continued convergence after geon 18 Penokean orogenesis: *Geological Society of America Bulletin*, v. 117,
639 p. 259, doi:10.1130/b25395.1.
- 640 Hrncir, J., Karlstrom, K., and Dahl, P., 2017, Wyoming on the run—Toward final Paleoproterozoic assembly of
641 Laurentia: COMMENT: *Geology*, v. 45, p. e411–e411, doi:10.1130/g38826c.1.
- 642 Hunter, J. D., 2007, Matplotlib: A 2D graphics environment: *Computing in Science & Engineering*, v. 9, p. 90–95,
643 doi:10.1109/MCSE.2007.55.
- 644 Irving, E., 2004, Early Proterozoic geomagnetic field in western Laurentia: implications for paleolatitudes, local
645 rotations and stratigraphy: *Precambrian Research*, v. 129, p. 251–270, doi:10.1016/j.precamres.2003.10.002.
- 646 Irving, E. and McGlynn, J. C., 1979, Palaeomagnetism in the Coronation Geosyncline and arrangement of
647 continents in the middle Proterozoic: *Geophysical Journal International*, v. 58, p. 309–336,
648 doi:10.1111/j.1365-246X.1979.tb01027.x.
- 649 Irving, E. and Park, J. K., 1972, Hairpins and superintervals: *Canadian Journal of Earth Sciences*, v. 9, p.
650 1318–1324, doi:10.1139/e72-115.
- 651 Jones, J. V., Daniel, C. G., and Doe, M. F., 2015, Tectonic and sedimentary linkages between the Belt-Purcell basin
652 and southwestern Laurentia during the Mesoproterozoic, ca. 1.60–1.40 Ga: *Lithosphere*, v. 7, p. 465–472,
653 doi:10.1130/l438.1.
- 654 Karlstrom, K. E., Ahall, K.-I., Harlan, S. S., Williams, M. L., McLellan, J., and Geissman, J. W., 2001, Long-lived
655 (1.8–1.0 Ga) convergent orogen in southern Laurentia, its extensions to Australia and Baltica, and implications
656 for refining Rodinia: *Precambrian Research*, v. 111, p. 5–30, doi:10.1016/S0301-9268(01)00154-1.
- 657 Karlstrom, K. E. and Bowring, S. A., 1988, Early Proterozoic assembly of tectonostratigraphic terranes in
658 southwestern North America: *The Journal of Geology*, v. 96, p. 561–576, doi:10.1086/629252.

- 659 Kean, W., Williams, I., and Feeney, J., 1997, Magnetism of the Keweenawan age Chengwatana lava flows, northwest
660 Wisconsin: Geophysical Research Letters, v. 24, p. 1523–1526, doi:10.1029/97gl00993.
- 661 Kilian, T. M., Bleeker, W., Chamberlain, K., Evans, D. A. D., and Cousens, B., 2015, Palaeomagnetism,
662 geochronology and geochemistry of the Palaeoproterozoic Rabbit Creek and Powder River dyke swarms:
663 implications for Wyoming in supercraton Superia: Geological Society, London, Special Publications, v. 424, p.
664 15–45, doi:10.1144/sp424.7.
- 665 Kilian, T. M., Chamberlain, K. R., Evans, D. A., Bleeker, W., and Cousens, B. L., 2016, Wyoming on the
666 run—Toward final Paleoproterozoic assembly of Laurentia: Geology, v. 44, p. 863–866, doi:10.1130/g38042.1.
- 667 Korenaga, J., 2013, Initiation and evolution of plate tectonics on earth: Theories and observations: Annual Review
668 of Earth and Planetary Sciences, v. 41, p. 117–151, doi:10.1146/annurev-earth-050212-124208.
- 669 Kulakov, E. V., Smirnov, A. V., and Diehl, J. F., 2013, Paleomagnetism of ~1.09 Ga Lake Shore Traps (Keweenaw
670 Peninsula, Michigan): new results and implications: Canadian Journal of Earth Sciences, v. 50, p. 1085–1096,
671 doi:10.1139/cjes-2013-0003.
- 672 Levy, M. and Christie-Blick, N., Nicholas, 1991, Tectonic subsidence of the early Paleozoic passive continental
673 margin in eastern California and southern Nevada: Geological Society of America Bulletin, v. 103, p. 1590–1606,
674 doi:10.1130/0016-7606(1991)103<1590:tsotep>2.3.co;2.
- 675 Li, Z. X. et al., 2008, Assembly, configuration, and break-up history of Rodinia: A synthesis: Precambrian
676 Research, v. 160, p. 179–210, doi:10.1016/j.precamres.2007.04.021.
- 677 Macdonald, F., Halverson, G., Strauss, J., Smith, E., Cox, G., Sperling, E., and Roots, C., 2012, Early
678 Neoproterozoic basin formation in Yukon, Canada: Implications for the make-up and break-up of Rodinia:
679 Geoscience Canada, v. 39.
- 680 Macdonald, F. A., Schmitz, M. D., Crowley, J. L., Roots, C. F., Jones, D. S., Maloof, A. C., Strauss, J. V., Cohen,
681 P. A., Johnston, D. T., and Schrag, D. P., 2010, Calibrating the Cryogenian: Science, v. 327, p. 1241–1243,
682 doi:10.1126/science.1183325.
- 683 Maloof, A., Halverson, G., Kirschvink, J., Schrag, D., Weiss, B., and Hoffman, P., 2006, Combined paleomagnetic,
684 isotopic and stratigraphic evidence for true polar wander from the Neoproterozoic Akademikerbreen Group,
685 Svalbard, Norway: Geological Society of America Bulletin, v. 118, p. 1099–1124, doi:10.1130/B25892.1.
- 686 Marcussen, C. and Abrahamsen, N., 1983, Palaeomagnetism of the Proterozoic Zig-Zag Dal Basalt and the
687 Midsommerso Dolerites, eastern North Greenland: Geophysical Journal International, v. 73, p. 367–387,
688 doi:10.1111/j.1365-246x.1983.tb03321.x.
- 689 Martin, E. L., Collins, W. J., and Spencer, C. J., 2019, Laurentian origin of the Cuyania suspect terrane, western
690 Argentina, confirmed by Hf isotopes in zircon: GSA Bulletin, doi:10.1130/b35150.1.

- 691 McCausland, P. J. A., Hankard, F., Van der Voo, R., and Hall, C. M., 2011, Ediacaran paleogeography of
692 Laurentia: Paleomagnetism and 40Ar-39Ar geochronology of the 583 Ma Baie des Moutons syenite, Quebec:
693 Precambrian Research, v. 187, p. 58–78, doi:10.1016/j.precamres.2011.02.004.
- 694 McCausland, P. J. A., Van der Voo, R., and Hall, C. M., 2007, Circum-Iapetus paleogeography of the
695 Precambrian–Cambrian transition with a new paleomagnetic constraint from Laurentia: Precambrian Research,
696 v. 156, p. 125–152, doi:10.1016/j.precamres.2007.03.004.
- 697 McFarlane, C. R., 2015, A geochronological framework for sedimentation and Mesoproterozoic tectono-magmatic
698 activity in lower Belt–Purcell rocks exposed west of Kimberley, British Columbia: Canadian Journal of Earth
699 Sciences, v. 52, p. 444–465, doi:10.1139/cjes-2014-0215.
- 700 McGlynn, J. C., Hanson, G. N., Irving, E., and Park, J. K., 1974, Paleomagnetism and age of Nonacho Group
701 sandstones and associated Sparrow dikes, District of Mackenzie: Canadian Journal of Earth Sciences, v. 11, p.
702 30–42, doi:10.1139/e74-003.
- 703 McLelland, J. M., Selleck, B. W., and Bickford, M., 2010, Review of the Proterozoic evolution of the Grenville
704 Province, its Adirondack outlier, and the Mesoproterozoic inliers of the Appalachians: From Rodinia to Pangea:
705 The Lithotectonic Record of the Appalachian Region, p. 21–49, doi:10.1130/2010.1206(02).
- 706 McLelland, J. M., Selleck, B. W., and Bickford, M. E., 2013, Tectonic evolution of the Adirondack Mountains and
707 Grenville Orogen inliers within the USA: Geoscience Canada, v. 40, p. 318, doi:10.12789/geocanj.2013.40.022.
- 708 McMechan, M. E. and Price, R. A., 1982, Superimposed low-grade metamorphism in the Mount Fisher area,
709 southeastern British Columbia—implications for the East Kootenay orogeny: Canadian Journal of Earth
710 Sciences, v. 19, p. 476–489, doi:10.1139/e82-039.
- 711 Meert, J., der Voo, R. V., and Payne, T., 1994, Paleomagnetism of the Catoctin volcanic province: a new
712 Vendian-Cambrian apparent polar wander path for North America: Journal of Geophysical Research, v. 99, p.
713 4625–4641.
- 714 Meert, J. G. and Stuckey, W., 2002, Revisiting the paleomagnetism of the 1.476 Ga St. Francois Mountains igneous
715 province, Missouri: Tectonics, v. 21, doi:10.1029/2000tc001265.
- 716 Meredith, A. S., Collins, A. S., Williams, S. E., Pisarevsky, S., Foden, J. D., Archibald, D. B., Blades, M. L., Alessio,
717 B. L., Armistead, S., Plavsa, D., and et al., 2017, A full-plate global reconstruction of the Neoproterozoic:
718 Gondwana Research, v. 50, p. 84–134, doi:10.1016/j.gr.2017.04.001.
- 719 Met Office, 2010 - 2015, Cartopy: a cartographic python library with a matplotlib interface: Exeter, Devon, URL
720 <http://scitools.org.uk/cartopy>.

- 721 Middleton, R. S., Borradaile, G. J., Baker, D., and Lucas, K., 2004, Proterozoic diabase sills of northern Ontario:
722 Magnetic properties and history: *Journal of Geophysical Research: Solid Earth*, v. 109,
723 doi:10.1029/2003jb002581.
- 724 Mitchell, R. N., Bleeker, W., van Breemen, O., Lecheminant, T. N., Peng, P., Nilsson, M. K. M., and Evans, D.
725 A. D., 2014, Plate tectonics before 2.0 Ga: Evidence from paleomagnetism of cratons within supercontinent
726 Nuna: *American Journal of Science*, v. 314, p. 878–894, doi:10.2475/04.2014.03.
- 727 Mitchell, R. N., Hoffman, P. F., and Evans, D. A. D., 2010, Coronation loop resurrected: Oscillatory apparent polar
728 wander of orosirian (2.05–1.8†ga) paleomagnetic poles from slave craton: *Precambrian Research*, v. 179, p.
729 121–134.
- 730 Mitchell, R. N., Kilian, T. M., and Evans, D. A. D., 2012, Supercontinent cycles and the calculation of absolute
731 palaeolongitude in deep time: *Nature*, v. 482, p. 208–211, doi:10.1038/nature10800.
- 732 Müller, R. D., Cannon, J., Qin, X., Watson, R. J., Gurnis, M., Williams, S., Pfaffelmoser, T., Seton, M., Russell, S.
733 H. J., and Zahirovic, S., 2018, GPlates: Building a virtual earth through deep time: *Geochemistry, Geophysics,
734 Geosystems*, v. 19, p. 2243–2261, doi:10.1029/2018gc007584.
- 735 Murthy, G., Gower, C., Tubett, M., and Patzold, R., 1992, Paleomagnetism of Eocambrian Long Range dykes and
736 Double Mer Formation from Labrador, Canada: *Canadian Journal of Earth Sciences*, v. 29, p. 1224–1234,
737 doi:10.1139/e92-098.
- 738 Murthy, G. S., 1978, Paleomagnetic results from the Nain anorthosite and their tectonic implications: *Canadian
739 Journal of Earth Sciences*, v. 15, p. 516–525, doi:10.1139/e78-058.
- 740 Nesheim, T. O., Vervoort, J. D., McClelland, W. C., Gilotti, J. A., and Lang, H. M., 2012, Mesoproterozoic
741 syntectonic garnet within Belt Supergroup metamorphic tectonites: Evidence of Grenville-age metamorphism
742 and deformation along northwest Laurentia: *Lithos*, v. 134–135, p. 91–107, doi:10.1016/j.lithos.2011.12.008.
- 743 Palin, R. M. and White, R. W., 2015, Emergence of blueschists on Earth linked to secular changes in oceanic crust
744 composition: *Nature Geoscience*, v. 9, p. 60–64, doi:10.1038/ngeo2605.
- 745 Palmer, H., 1970, Paleomagnetism and correlation of some Middle Keweenawan rocks, Lake Superior: *Canadian
746 Journal of Earth Science*, v. 7, p. 1410–1436, doi:10.1139/e70-136.
- 747 Palmer, H. C., Merz, B. A., and Hayatsu, A., 1977, The Sudbury dikes of the Grenville Front region:
748 paleomagnetism, petrochemistry, and K–Ar age studies: *Canadian Journal of Earth Sciences*, v. 14, p. 1867–1887.
- 749 Park, J. K., Irving, E., and Donaldson, J. A., 1973, Paleomagnetism of the Precambrian Dubawnt Group:
750 Geological Society of America Bulletin, v. 84, p. 859, doi:10.1130/0016-7606(1973)84<859:potpdg>2.0.co;2.

- 751 Pehrsson, S. J., Eglington, B. M., Evans, D. A. D., Huston, D., and Reddy, S. M., 2015, Metallogeny and its link to
752 orogenic style during the Nuna supercontinent cycle: Geological Society, London, Special Publications, v. 424,
753 doi:10.1144/SP424.5.
- 754 Pérez, F. and Granger, B. E., 2007, IPython: a system for interactive scientific computing: Computing in Science
755 and Engineering, v. 9, p. 21–29, doi:10.1109/MCSE.2007.53.
- 756 Pesonen, L., 1979, Paleomagnetism of late Precambrian Keweenawan igneous and baked contact rocks from
757 Thunder Bay district, northern Lake Superior: Bulletin of the Geological Society of Finland, v. 51, p. 27–44.
- 758 Pesonen, L. J. and Halls, H., 1979, The paleomagnetism of Keweenawan dikes from Baraga and Marquette
759 Counties, northern Michigan: Canadian Journal of Earth Science, v. 16, p. 2136–2149, doi:10.1139/e79-201.
- 760 Piispa, E. J., Smirnov, A. V., Pesonen, L. J., and Mitchell, R. H., 2018, Paleomagnetism and geochemistry of
761 1144-ma lamprophyre dikes, Northwestern Ontario: Implications for the North American polar wander and plate
762 velocities: Journal of Geophysical Research: Solid Earth, doi:10.1029/2018jb015992.
- 763 Piper, J., 1992, The palaeomagnetism of major (Middle Proterozoic) igneous complexes, South Greenland and the
764 Gardar apparent polar wander track: Precambrian Research, v. 54, p. 153 – 172,
765 doi:10.1016/0301-9268(92)90068-Y.
- 766 Piper, J. and Stearn, J., 1977, Palaeomagnetism of the dyke swarms of the Gardar Igneous Province, south
767 Greenland: Physics of the Earth and Planetary Interiors, v. 14, p. 345–358, doi:10.1016/0031-9201(77)90167-4.
- 768 Piper, J. D. A., 1977, Palaeomagnetism of the giant dykes of Tugtutoq and Narssaq Gabbro, Gardar Igneous
769 Province, South Greenland: Bull. Geol. Soc. Den, v. 26, p. 85–94.
- 770 Pisarevsky, S. A., Elming, S.-Å., Pesonen, L. J., and Li, Z.-X., 2014, Mesoproterozoic paleogeography:
771 Supercontinent and beyond: Precambrian Research, v. 244, p. 207–225, doi:10.1016/j.precamres.2013.05.014.
- 772 Pullaiah, G. and Irving, E., 1975, Paleomagnetism of the contact aureole and late dikes of the Otto stock, Ontario,
773 and its application to early proterozoic apparent polar wandering: Canadian Journal of Earth Sciences, v. 12, p.
774 1609–1618, doi:10.1139/e75-143.
- 775 Rapalini, A. E., 2018, The assembly of western Gondwana: Reconstruction based on paleomagnetic data: Geology
776 of Southwest Gondwana, p. 3–18, doi:10.1007/978-3-319-68920-3_1.
- 777 Redden, J., Peterman, Z., Zartman, R., and De-Witt, E., 1990, U-Th-Pb geochronology and preliminary
778 interpretation of Precambrian tectonic events in the Black Hills, South Dakota: *In* The Early Proterozoic
779 Trans-Hudson Orogen, Geological Association of Canada Special Paper 37, p. 229–251.
- 780 Rivers, T., 2008, Assembly and preservation of lower, mid, and upper orogenic crust in the Grenville
781 Province—implications for the evolution of large hot long-duration orogens: Precambrian Research, v. 167, p.
782 237–259, doi:10.1016/j.precamres.2008.08.005.

- 783 Robert, B., Besse, J., Blein, O., Greff-Lefftz, M., Baudin, T., Lopes, F., Meslouh, S., and Belbadaoui, M., 2017,
784 Constraints on the ediacaran inertial interchange true polar wander hypothesis: A new paleomagnetic study in
785 morocco (west african craton): Precambrian Research, v. 295, p. 90–116, doi:10.1016/j.precamres.2017.04.010.
- 786 Robertson, W. and Fahrig, W., 1971, The great Logan Loop - the polar wandering path from Canadian shield rocks
787 during the Neohelikian era: Canadian Journal of Earth Science, v. 8, p. 1355–1372, doi:10.1139/e71-125.
- 788 Roest, W. R. and Srivastava, S. P., 1989, Sea-floor spreading in the labrador sea: A new reconstruction: Geology,
789 v. 17, p. 1000, doi:10.1130/0091-7613(1989)017<1000:sfsitl>2.3.co;2.
- 790 Rooney, A. D., Austermann, J., Smith, E. F., Li, Y., Selby, D., Dehler, C. M., Schmitz, M. D., Karlstrom, K. E.,
791 and Macdonald, F. A., 2017, Coupled Re-Os and U-Pb geochronology of the Tonian Chuar Group, Grand
792 Canyon: GSA Bulletin, doi:10.1130/b31768.1.
- 793 Ross, G. M., 1991, Tectonic setting of the Windermere Supergroup revisited: Geology, v. 19, p. 1125,
794 doi:10.1130/0091-7613(1991)019<1125:tsotws>2.3.co;2.
- 795 Schmidt, P. W., 1980, Paleomagnetism of igneous rocks from the Belcher Islands, Northwest Territories, Canada:
796 Canadian Journal of Earth Sciences, v. 17, p. 807–822, doi:10.1139/e80-081.
- 797 Schulz, K. J. and Cannon, W. F., 2007, The Penokean orogeny in the Lake Superior region: Precambrian Research,
798 v. 157, p. 4–25, doi:10.1016/j.precamres.2007.02.022.
- 799 Schwarz, E. J., Clark, K. R., and Fujiwara, Y., 1982, Paleomagnetism of the Sutton Lake Proterozoic inlier,
800 Ontario, Canada: Canadian Journal of Earth Sciences, v. 19, p. 1330–1332, doi:10.1139/e82-114.
- 801 Selkin, P. A., Gee, J. S., Meurer, W. P., and Hemming, S. R., 2008, Paleointensity record from the 2.7 Ga Stillwater
802 Complex, Montana: Geochem. Geophys. Geosyst., v. 9, p. 10.1029/2008GC001,950.
- 803 Skipton, D. R., St-Onge, M. R., Schneider, D. A., and McFarlane, C. R. M., 2016, Tectonothermal evolution of the
804 middle crust in the Trans-Hudson Orogen, Baffin Island, Canada: Evidence from petrology and monazite
805 geochronology of sillimanite-bearing migmatites: Journal of Petrology, v. 57, p. 1437–1462,
806 doi:10.1093/petrology/egw046.
- 807 Slagstad, T., Culshaw, N. G., Daly, J. S., and Jamieson, R. A., 2009, Western Grenville Province holds key to
808 midcontinental Granite-Rhyolite Province enigma: Terra Nova, v. 21, p. 181–187,
809 doi:10.1111/j.1365-3121.2009.00871.x.
- 810 St-Onge, M. R., Van Gool, J. A. M., Garde, A. A., and Scott, D. J., 2009, Correlation of Archaean and
811 Palaeoproterozoic units between northeastern Canada and western Greenland: constraining the pre-collisional
812 upper plate accretionary history of the Trans-Hudson orogen: Geological Society, London, Special Publications,
813 v. 318, p. 193–235, doi:10.1144/sp318.7.

- 814 Stern, R. J. and Miller, N. R., 2018, Did the transition to plate tectonics cause neoproterozoic snowball earth?:
815 *Terra Nova*, v. 30, p. 87–94, doi:10.1111/ter.12321.
- 816 Stern, R. J., Tsujimori, T., Harlow, G., and Groat, L. A., 2013, Plate tectonic gemstones: *Geology*, v. 41, p.
817 723–726, doi:10.1130/g34204.1.
- 818 Swanson-Hysell, N. L., Burgess, S. D., Maloof, A. C., and Bowring, S. A., 2014a, Magmatic activity and plate
819 motion during the latent stage of Midcontinent Rift development: *Geology*, v. 42, p. 475–478,
820 doi:10.1130/G35271.1.
- 821 Swanson-Hysell, N. L., Ramezani, J., Fairchild, L. M., and Rose, I. R., 2019, Failed rifting and fast drifting:
822 Midcontinent Rift development, Laurentia's rapid motion and the driver of Grenvillian orogenesis: *GSA Bulletin*,
823 doi:10.1130/b31944.1.
- 824 Swanson-Hysell, N. L., Vaughan, A. A., Mustain, M. R., and Asp, K. E., 2014b, Confirmation of progressive plate
825 motion during the Midcontinent Rift's early magmatic stage from the Osler Volcanic Group, Ontario, Canada:
826 *Geochemistry Geophysics Geosystems*, v. 15, p. 2039–2047, doi:10.1002/2013GC005180.
- 827 Symons, D. and Chiasson, A., 1991, Paleomagnetism of the Callander Complex and the Cambrian apparent polar
828 wander path for North America: *Canadian Journal of Earth Science*, v. 1991, p. 355–363, doi:10.1139/e91-032.
- 829 Symons, D., Symons, T., and Lewchuk, M., 2000, Paleomagnetism of the Deschambault pegmatites: Stillstand and
830 hairpin at the end of the Paleoproterozoic Trans-Hudson Orogeny, Canada: *Physics and Chemistry of the Earth*,
831 Part A: Solid Earth and Geodesy, v. 25, p. 479–487, doi:10.1016/s1464-1895(00)00074-0.
- 832 Symons, D. T. A. and Mackay, C. D., 1999, Paleomagnetism of the Boot-Phantom pluton and the amalgamation of
833 the juvenile domains in the Paleoproterozoic Trans-Hudson Orogen, Canada: In Sinha, A. K., ed., *Basement
834 Tectonics 13*, Springer Netherlands, Dordrecht, p. 313–331, doi:10.1007/978-94-011-4800-9_{_}18.
- 835 Tanczyk, E., Lapointe, P., Morris, W., and Schmidt, P., 1987, A paleomagnetic study of the layered mafic intrusions
836 at Sept-Iles, Quebec: *Canadian Journal of Earth Science*, v. 24, p. 1431–1438, doi:10.1139/e87-135.
- 837 Tauxe, L. and Kodama, K., 2009, Paleosecular variation models for ancient times: Clues from Keweenawan lava
838 flows: *Physics of the Earth and Planetary Interiors*, v. 177, p. 31–45, doi:10.1016/j.pepi.2009.07.006.
- 839 Tauxe, L., Shaar, R., Jonestrask, L., Swanson-Hysell, N., Minnett, R., Koppers, A., Constable, C., Jarboe, N.,
840 Gaastra, K., and Fairchild, L., 2016, PmagPy: Software package for paleomagnetic data analysis and a bridge to
841 the Magnetics Information Consortium (MagIC) Database: *Geochemistry, Geophysics, Geosystems*,
842 doi:10.1002/2016GC006307.
- 843 Torsvik, T. H. and Cocks, L. R. M., 2017, Earth history and palaeogeography: Cambridge University Press,
844 doi:10.1017/9781316225523.

- 845 Torsvik, T. H., van der Voo, R., Doubrovine, P. V., Burke, K., Steinberger, B., Ashwal, L. D., Trønnes, R. G.,
846 Webb, S. J., and Bull, A. L., 2014, Deep mantle structure as a reference frame for movements in and on the
847 Earth: *Proceedings of the National Academy of Sciences*, doi:10.1073/pnas.1318135111.
- 848 Torsvik, T. H., Van der Voo, R., Preeden, U., Mac Niocaill, C., Steinberger, B., Doubrovine, P. V., van Hinsbergen,
849 D. J. J., Domeier, M., Gaina, C., Tohver, E., Meert, J. G., McCausland, P. J. A., and Cocks, L. R. M., 2012,
850 Phanerozoic polar wander, palaeogeography and dynamics: *Earth-Science Reviews*, v. 114, p. 325–368,
851 doi:10.1016/j.earscirev.2012.06.007.
- 852 Veikkolainen, T., Pesonen, L., and Evans, D. D., 2014, PALEOMAGIA: A PHP/MYSQL database of the
853 Precambrian paleomagnetic data: p. 1–17, doi:10.1007/s11200-013-0382-0.
- 854 Warnock, A., Kodama, K., and Zeitler, P., 2000, Using thermochronometry and low-temperature demagnetization
855 to accurately date Precambrian paleomagnetic poles: *Journal of Geophysical Research*, v. 105, p. 19,435–19,453,
856 doi:10.1029/2000jb900114.
- 857 Weil, A., Geissman, J., Heizler, M., and Van der Voo, R., 2003, Paleomagnetism of Middle Proterozoic mafic
858 intrusions and Upper Proterozoic (Nankoweap) red beds from the Lower Grand Canyon Supergroup, Arizona:
859 *Tectonophysics*, v. 375, p. 199–220, doi:10.1016/S0040-1951(03)00339-1.
- 860 Weil, A. B., Geissman, J. W., and Ashby, J. M., 2006, A new paleomagnetic pole for the Neoproterozoic Uinta
861 Mountain supergroup, Central Rocky Mountain States, USA: *Precambrian Research*, v. 147, p. 234–259,
862 doi:10.1016/j.precamres.2006.01.017.
- 863 Weil, A. B., Geissman, J. W., and Voo, R. V. d., 2004, Paleomagnetism of the Neoproterozoic Chuar Group, Grand
864 Canyon Supergroup, Arizona: implications for Laurentia's Neoproterozoic APWP and Rodinia break-up:
865 *Precambrian Research*, v. 129, p. 71–92.
- 866 Weller, O. M. and St-Onge, M. R., 2017, Record of modern-style plate tectonics in the Palaeoproterozoic
867 Trans-Hudson orogen: *Nature Geoscience*, v. 10, doi:10.1038/ngeo2904.
- 868 Whitmeyer, S. and Karlstrom, K., 2007, Tectonic model for the Proterozoic growth of North America: *Geosphere*,
869 v. 3, p. 220–259, doi:10.1130/GES00055.1.
- 870 Witkosky, R. and Wernicke, B. P., 2018, Subsidence history of the Ediacaran Johnnie Formation and related strata
871 of southwest Laurentia: Implications for the age and duration of the Shuram isotopic excursion and animal
872 evolution: *Geosphere*, v. 14, p. 2245–2276, doi:10.1130/ges01678.1.
- 873 Zhang, S., Li, Z.-X., Evans, D. A. D., Wu, H., Li, H., and Dong, J., 2012, Pre-Rodinia supercontinent Nuna shaping
874 up: A global synthesis with new paleomagnetic results from North China: *Earth and Planetary Science Letters*,
875 v. 353–354, p. 145–155.

Table 1. Rotations of separated terranes

Block	Euler pole longitude	Euler pole latitude	rotation angle	note and citation
Greenland	-118.5	67.5	-13.8	Cenozoic separation of Greenland from Laurentia associated with opening of Baffin Bay and the Labrador Sea (Roest and Srivastava, 1989)
Scotland	161.9	78.6	-31.0	Reconstructing Atlantic opening following Torsvik and Cocks (2017)
Svalbard	125.0	-81.0	68	Rotate Svalbard to Laurentia in fit that works well with East Greenland basin according to Maloof et al. (2006)

876

Table 2: Compilation of paleomagnetic poles from Laurentia

terrane	unit name	Nordic rating	site lon (°)	site lat (°)	plon (°)	plat (°)	A ₉₅ (°)	age (Ma)	pole reference
Laurentia-Wyoming	Stillwater Complex - C2	A	249.2	45.2	335.8	-83.6	4.0	2705 ⁺⁴ ₋₄	Selkin et al. (2008)
Laurentia-Superior(East)	Otto Stock dykes and aureole	B	279.9	48.0	227.0	69.0	4.8	2676 ⁺⁵ ₋₅	Pullaiah and Irving (1975)
Laurentia-Slave	Defeat Suite	B	245.5	62.5	64.0	-1.0	15.0	2625 ⁺⁵ ₋₅	Mitchell et al. (2014)
Laurentia-Superior(East)	Ptarmigan-Mistassini dykes	B	287.0	54.0	213.0	-45.3	13.8	2505 ⁺² ₋₂	Evans and Halls (2010)
Laurentia-Superior(East)	Matachewan dykes	A	278.0	48.0	238.3	-44.1	1.6	2466 ⁺²³ ₋₂₃	Evans and Halls (2010)
Laurentia-Superior(East)	Matachewan dykes N	A	278.0	48.0	239.5	-52.3	2.4	2446 ⁺³ ₋₃	Evans and Halls (2010)
Laurentia-Slave	Malley dykes	A	249.8	64.2	310.0	-50.8	6.7	2231 ⁺² ₋₂	Buchan et al. (2012)
Laurentia-Superior(East)	Senneterre dykes	A	283.0	49.0	284.3	-15.3	5.5	2218 ⁺⁶ ₋₆	Buchan et al. (1993)
Laurentia-Superior(East)	Nipissing N1 sills	A	279.0	47.0	272.0	-17.0	10.0	2217 ⁺⁴ ₋₄	Buchan et al. (2000)
Laurentia-Slave	Dogrib dykes	A	245.5	62.5	315.0	-31.0	7.0	2193 ⁺² ₋₂	Mitchell et al. (2014)
Laurentia-Superior(East)	Biscotasing dykes	A	280.0	48.0	223.9	26.0	7.0	2170 ⁺³ ₋₃	Evans and Halls (2010)
Laurentia-Wyoming	Rabbit Creek, Powder River and South Path Dykes	A	252.8	43.9	339.2	65.5	7.6	2160 ⁺¹¹ ₋₈	Kilian et al. (2015)
Laurentia-Slave	Indin dykes	A	245.6	62.5	256.0	-36.0	7.0	2126 ⁺³ ₋₁₈	Buchan et al. (2016)
Laurentia-Superior(West)	Marathon dykes N	A	275.0	49.0	198.2	45.4	7.7	2124 ⁺³ ₋₃	Halls et al. (2008)

Continued on next page

terrane	unit name	Nordic rating	site lon (°)	site lat (°)	plon (°)	plat (°)	A ₉₅ (°)	age (Ma)	pole reference
Laurentia-Superior(West)	Marathon dykes R	A	275.0	49.0	182.2	55.1	7.5	2104 ⁺³ ₋₃	Halls et al. (2008)
Laurentia-Superior(West)	Cauchon Lake dykes	A	263.0	56.0	180.9	53.8	7.7	2091 ⁺² ₋₂	Evans and Halls (2010)
Laurentia-Superior(West)	Fort Frances dykes	A	266.0	48.0	184.6	42.8	6.1	2077 ⁺⁵ ₋₅	Evans and Halls (2010)
Laurentia-Superior(East)	Lac Esprit dykes	A	282.0	53.0	170.5	62.0	6.4	2069 ⁺¹ ₋₁	Evans and Halls (2010)
Laurentia-Greenland-Nain	Kangamiut Dykes	B	307.0	66.0	273.8	17.1	2.7	2042 ⁺¹² ₋₁₂	Fahrig and Bridgwater (1976)
Laurentia-Slave	Lac de Gras dykes	A	249.6	64.4	267.9	11.8	7.1	2026 ⁺⁵ ₋₅	Buchan et al. (2009)
Laurentia-Superior(East)	Minto dykes	A	285.0	57.0	171.5	38.7	13.1	1998 ⁺² ₋₂	Evans and Halls (2010)
Laurentia-Slave	Rifle Formation	B	252.9	65.9	341.0	14.0	7.7	1963 ⁺⁶ ₋₆	Evans and Hoye (1981)
Laurentia-Rae	Clearwater Anorthosite	B	251.6	57.1	311.8	6.5	2.9	1917 ⁺⁷ ₋₇	Halls and Hanes (1999)
Laurentia-Wyoming	Sourdough mafic dike swarm	A	-108.3	44.7	292.0	49.2	8.1	1899 ⁺⁵ ₋₅	Kilian et al. (2016)
Laurentia-Slave	Ghost Dike Swarm	A	244.6	62.6	286.0	-2.0	6.0	1887 ⁺⁵ ₋₉	Buchan et al. (2016)
Laurentia-Slave	Mean Se-ton/Akaitcho/Mara	B	250.0	65.0	260.0	-6.0	4.0	1885 ⁺⁵ ₋₅	Mitchell et al. (2010)
Laurentia-Slave	Mean Kahochella, Peacock Hills	B	250.0	65.0	285.0	-12.0	7.0	1882 ⁺⁴ ₋₄	Mitchell et al. (2010)
Laurentia-Superior(West)	Molson (B+C2) dykes	A	262.0	55.0	218.0	28.9	3.8	1879 ⁺⁶ ₋₆	Evans and Halls (2010)

Continued on next page

terrane	unit name	Nordic rating	site lon (°)	site lat (°)	plon (°)	plat (°)	A ₉₅ (°)	age (Ma)	pole reference
Laurentia-Slave	Douglas Peninsula Formation, Pethei Group	B	249.7	62.8	258.0	-18.0	14.2	1876 ⁺¹⁰ ₋₁₀	Irving and McGlynn (1979)
Laurentia-Slave	Takiyuak Formation	B	246.9	66.1	249.0	-13.0	8.0	1876 ⁺¹⁰ ₋₁₀	Irving and McGlynn (1979)
Laurentia-Superior	Haig/Flaherty/Sutton Mean	B	279.0	56.0	245.8	1.0	3.9	1870 ⁺¹ ₋₁	Nordic workshop calculation based on data of Schmidt (1980); Schwarz et al. (1982)
Laurentia-Slave	Pearson A/Peninsular/Kilohigok sills	A	250.0	65.0	269.0	-22.0	6.0	1870 ⁺⁴ ₋₄	Mitchell et al. (2010)
Laurentia-Trans-Hudson orogen	Boot-Phantom Pluton	B	258.1	54.7	275.4	62.4	7.9	1838 ⁺¹ ₋₁	Symons and Mackay (1999)
Laurentia-Rae	Sparrow Dykes	B	250.2	61.6	291.0	12.0	7.9	1827 ⁺⁴ ₋₄	McGlynn et al. (1974)
Laurentia-Rae	Martin Formation	A	251.4	59.6	288.0	-9.0	8.5	1818 ⁺⁴ ₋₄	Evans and Bingham (1973)
Laurentia	Dubawnt Group	B	265.6	64.1	277.0	7.0	8.0	1785 ⁺³⁵ ₋₃₅	Park et al. (1973)
Laurentia-Trans-Hudson orogen	Deschambault Pegmatites	B	256.7	54.9	276.0	67.5	7.7	1766 ⁺⁵ ₋₅	Symons et al. (2000)
Laurentia-Trans-Hudson orogen	Jan Lake Granite	B	257.2	54.9	264.3	24.3	16.9	1758 ⁺¹ ₋₁	Gala et al. (1995)
Laurentia	Cleaver Dykes	A	242.0	67.5	276.7	19.4	6.1	1741 ⁺⁵ ₋₅	Irving (2004)
Laurentia-Greenland	Melville Bugt dia-base dykes	B	303.0	74.6	273.8	5.0	8.7	1633 ⁺⁵ ₋₅	Halls et al. (2011)
Laurentia	Western Channel Diabase	A	242.2	66.4	245.0	9.0	6.6	1590 ⁺³ ₋₃	Irving and Park (1972)

Continued on next page

terrane	unit name	Nordic rating	site lon (°)	site lat (°)	plon (°)	plat (°)	A ₉₅ (°)	age (Ma)	pole reference
Laurentia	St.Francois Mountains Acidic Rocks	A	269.5	37.5	219.0	-13.2	6.1	1476 ⁺¹⁶ ₋₁₆	Meert and Stuckey (2002)
Laurentia	Michikamau Intrusion	A	296.0	54.5	217.5	-1.5	4.7	1460 ⁺⁵ ₋₅	Emslie et al. (1976)
Laurentia	Spokane Formation	A	246.8	48.2	215.5	-24.8	4.7	1458 ⁺¹³ ₋₁₃	Elston et al. (2002)
Laurentia	Snowslip Formation	A	245.9	47.9	210.2	-24.9	3.5	1450 ⁺¹⁴ ₋₁₄	Elston et al. (2002)
Laurentia	Tobacco Root dykes	B	247.6	47.4	216.1	8.7	10.5	1448 ⁺⁴⁹ ₋₄₉	Harlan et al. (2008)
Laurentia	Purcell Lava	A	245.1	49.4	215.6	-23.6	4.8	1443 ⁺⁷ ₋₇	Elston et al. (2002)
Laurentia	Rocky Mountain intrusions	B	253.8	40.3	217.4	-11.9	9.7	1430 ⁺¹⁵ ₋₁₅	Nordic workshop calculation based on data of Harlan et al. (1994); Harlan and Geissman (1998)
Laurentia	Mistastin Pluton	B	296.3	55.6	201.5	-1.0	7.6	1425 ⁺²⁵ ₋₂₅	Fahrig and Jones (1976)
Laurentia	McNamara Formation	A	246.4	46.9	208.3	-13.5	6.7	1401 ⁺⁶ ₋₆	Elston et al. (2002)
Laurentia	Pilcher, Garnet Range and Libby Formations	A	246.4	46.7	215.3	-19.2	7.7	1385 ⁺²³ ₋₂₃	Elston et al. (2002)
Laurentia-Greenland	Zig-Zag Dal Basalts	B	334.8	81.2	242.8	12.0	3.8	1382 ⁺² ₋₂	Marcussen and Abrahamsen (1983)
Laurentia-Greenland	Midsommersoe Dolerite	B	333.4	81.6	242.0	6.9	5.1	1382 ⁺² ₋₂	Marcussen and Abrahamsen (1983)
Laurentia-Greenland	Victoria Fjord dolerite dykes	B	315.3	81.5	231.7	10.3	4.3	1382 ⁺² ₋₂	Abrahamsen and Van Der Voo (1987)

Continued on next page

terrane	unit name	Nordic rating	site lon (°)	site lat (°)	plon (°)	plat (°)	A_{95} (°)	age (Ma)	pole reference
Laurentia	Nain Anorthosite	B	298.2	56.5	206.7	11.7	2.2	1305^{+15}_{-15}	Murthy (1978)
Laurentia-Greenland	North Qoroq intrusives	B	314.6	61.1	202.6	13.2	8.3	1275^{+1}_{-1}	Piper (1992)
Laurentia-Greenland	Kungnat Ring Dyke	B	311.7	61.2	198.7	3.4	3.2	1275^{+2}_{-2}	Piper and Stearn (1977)
Laurentia	Mackenzie dykes	A	250.0	65.0	190.0	4.0	5.0	1267^{+2}_{-2}	Buchan et al. (2000)
	grand mean								
Laurentia-Greenland	West Gardar Dolerite Dykes	B	311.7	61.2	201.7	8.7	6.6	1244^{+8}_{-8}	Piper and Stearn (1977)
Laurentia-Greenland	West Gardar Lamprophyre Dykes	B	311.7	61.2	206.4	3.2	7.2	1238^{+11}_{-11}	Piper and Stearn (1977)
Laurentia	Sudbury Dykes	A	278.6	46.3	192.8	-2.5	2.5	1237^{+5}_{-5}	Palmer et al. (1977)
	Combined								
Laurentia-Scotland	Stoer Group	B	354.5	58.0	238.4	37.2	7.7	1199^{+70}_{-70}	Nordic workshop calculation
Laurentia-Greenland	Narssaq Gabbro	B	313.8	60.9	225.4	31.6	9.7	1184^{+5}_{-5}	Piper (1977)
Laurentia-Greenland	Hviddal Giant Dyke	B	313.7	60.9	215.3	33.2	9.6	1184^{+5}_{-5}	Piper (1977)
Laurentia-Greenland	South Qoroq Intr.	A	314.6	61.1	215.9	41.8	13.1	1163^{+2}_{-2}	Piper (1992)
Laurentia-Greenland	Giant Gabbro Dykes	B	313.7	60.9	226.1	42.3	9.4	1163^{+2}_{-2}	Piper (1977)
Laurentia-Greenland	NE-SW Trending dykes	B	314.6	61.1	230.8	33.4	5.7	1160^{+5}_{-5}	Piper (1992)
Laurentia	Ontario lamprophyre dykes	NR	273.3	48.8	223.3	58.0	9.2	1143^{+10}_{-10}	Piispa et al. (2018)

Continued on next page

terrane	unit name	Nordic rating	site lon (°)	site lat (°)	plon (°)	plat (°)	A_{95} (°)	age (Ma)	pole reference
Laurentia	Abitibi Dykes	A	279.0	48.0	215.5	48.8	14.1	1141^{+2}_{-2}	Ernst and Buchan (1993)
Laurentia	Nipigon sills and lavas	A	270.9	49.1	217.8	47.2	4.0	1109^{+2}_{-2}	Nordic workshop calculation based on data of Palmer (1970); Robertson and Fahrig (1971); Pesonen (1979); Pesonen and Halls (1979); Middleton et al. (2004); Borradaile and Middleton (2006)
Laurentia	Lowermost Mamainse Point volcanics -R1	A	275.3	47.1	227.0	49.5	5.3	1109^{+2}_{-3}	Swanson-Hysell et al. (2014a)
Laurentia	Lower Osler volcanics -R	A	272.3	48.8	218.6	40.9	4.8	1108^{+3}_{-3}	Swanson-Hysell et al. (2014b)
Laurentia	Middle Osler volcanics -R	A	272.4	48.8	211.3	42.7	8.2	1107^{+4}_{-4}	Swanson-Hysell et al. (2014b)
Laurentia	Upper Osler volcanics -R	A	272.4	48.7	203.4	42.3	3.7	1105^{+1}_{-1}	Halls (1974); Swanson-Hysell et al. (2014b, 2019)
Laurentia	Lower Mamainse Point volcanics -R2	A	275.3	47.1	205.2	37.5	4.5	1105^{+3}_{-4}	Swanson-Hysell et al. (2014a)
Laurentia	Mamainse Point volcanics -C (lower N, upper R)	A	275.3	47.1	189.7	36.1	4.9	1101^{+1}_{-1}	Swanson-Hysell et al. (2014a)
Laurentia	North Shore lavas -N	A	268.7	46.3	181.7	31.1	2.1	1097^{+3}_{-3}	Tauxe and Kodama (2009); Swanson-Hysell et al. (2019)

Continued on next page

terrane	unit name	Nordic rating	site lon (°)	site lat (°)	plon (°)	plat (°)	A ₉₅ (°)	age (Ma)	pole reference
Laurentia	Portage Lake Volcanics	A	271.2	47.0	182.5	27.5	2.3	1095 ₋₃ ⁺³	Books (1972); Hnat et al. (2006) as calculated in Swanson-Hysell et al. (2019)
Laurentia	Chengwatana Volcanics	B	267.3	45.4	186.1	30.9	8.2	1095 ₋₂ ⁺²	Kean et al. (1997)
Laurentia	Uppermost Mainse Point volcanics -N	A	275.3	47.1	183.2	31.2	2.5	1094 ₋₄ ⁺⁶	Swanson-Hysell et al. (2014a)
Laurentia	Cardenas Basalts and Intrusions	B	248.1	36.1	185.0	32.0	8.0	1091 ₋₅ ⁺⁵	Weil et al. (2003)
Laurentia	Schroeder Lutsen Basalts	A	269.1	47.5	187.8	27.1	3.0	1090 ₋₇ ⁺²	Fairchild et al. (2017)
Laurentia	Central Arizona diabases -N	A	249.2	33.7	175.3	15.7	7.0	1088 ₋₁₁ ⁺¹¹	Donadini et al. (2011)
Laurentia	Lake Shore Traps	A	271.9	47.6	186.4	23.1	4.0	1086 ₋₁ ⁺¹	Kulakov et al. (2013)
Laurentia	Michipicoten Island Formation	A	274.3	47.7	174.7	17.0	4.4	1084 ₋₁ ⁺¹	Fairchild et al. (2017)
Laurentia	Nonesuch Shale	B	271.5	47.0	178.1	7.6	5.5	1080 ₋₁₀ ⁺⁴	Henry et al. (1977)
Laurentia	Freda Sandstone	B	271.5	47.0	179.0	2.2	4.2	1070 ₋₁₀ ⁺¹⁴	Henry et al. (1977)
Laurentia	Haliburton Intrusions	B	281.4	45.0	141.9	-32.6	6.3	1015 ₋₁₅ ⁺¹⁵	Warnock et al. (2000)
Laurentia-Scotland	Torridon Group	B	354.3	57.9	220.9	-17.7	7.1	925 ₋₁₄₅ ⁺¹⁴⁵	Nordic workshop calculation
Laurentia-Svalbard	Lower Grusdievbreen Formation	B	18.0	79.0	204.9	19.6	10.9	831 ₋₂₀ ⁺²⁰	Maloof et al. (2006)

Continued on next page

terrane	unit name	Nordic rating	site lon (°)	site lat (°)	plon (°)	plat (°)	A ₉₅ (°)	age (Ma)	pole reference
Laurentia-Svalbard	Upper Grus-dievbreen Formation	B	18.2	78.9	252.6	-1.1	6.2	800 ⁺¹¹ ₋₁₁	Maloof et al. (2006)
Laurentia	Gunbarrel dykes	B	248.7	44.8	138.2	9.1	12.0	778 ⁺² ₋₂	Calculation from Eyster et al. (2019) based on data of Harlan (1993); Harlan et al. (1997)
Laurentia-Svalbard	Svanbergfjellet Formation	B	18.0	78.5	226.8	25.9	5.8	770 ⁺¹⁹ ₋₄₀	Maloof et al. (2006)
Laurentia	Uinta Mountain Group	B	250.7	40.8	161.3	0.8	4.7	760 ⁺⁶ ₋₁₀	Weil et al. (2006)
Laurentia	Carbon Canyon	NR	248.2	36.1	166.0	-0.5	9.7	757 ⁺⁷ ₋₇	Weil et al. (2004) as calculated in Eyster et al. (2019)
Laurentia	Carbon Butte/Awatubi	NR	248.5	35.2	163.8	14.2	3.5	751 ⁺⁸ ₋₈	Eyster et al. (2019)
Laurentia	Franklin event grand mean	A	275.4	73.0	162.1	6.7	3.0	724 ⁺³ ₋₃	Denyszyn et al. (2009a)
Laurentia	Long Range Dykes	B	303.3	53.7	355.3	19.0	17.4	615 ⁺² ₋₂	Murthy et al. (1992)
Laurentia	Baie des Moutons complex	B	301.0	50.8	321.5	-34.2	15.4	583 ⁺² ₋₂	McCausland et al. (2011)
Laurentia	Baie des Moutons complex	B	301.0	50.8	332.7	42.6	12.0	583 ⁺² ₋₂	McCausland et al. (2011)
Laurentia	Callander Alkaline Complex	B	280.6	46.2	301.4	46.3	6.0	575 ⁺⁵ ₋₅	Symons and Chiasson (1991)
Laurentia	Catoctin Basalts	B	281.8	38.5	296.7	42.0	17.5	572 ⁺⁵ ₋₅	Meert et al. (1994)

Continued on next page

terrane	unit name	Nordic rating	site lon (°)	site lat (°)	plon (°)	plat (°)	A ₉₅ (°)	age (Ma)	pole reference
Laurentia	Sept-Iles layered intrusion	B	293.5	50.2	321.0	-20.0	6.7	565 ⁺⁴ ₋₄	Tanczyk et al. (1987)